Mechanical Hip Prosthetic

Final Report

Aiden Camisa | Team Lead, Controls Integration (LabView)

Victoria Lyon | Operations & Budget Manager, Mechanical Systems

Matthew Martinez | Manufacturing Lead, Biomechanics & Anatomical Design

Quinn O'Neill | Embedded Systems & Motor Control (C++), Website Design Lead

Fall 2025-Spring 2026

Project Sponsor: NextStep Prosthetics

Faculty Advisor & Sponsor Mentor: Dr. Dante Archangeli, Dr. Reza Razavian

Instructor: Professor David Willy

DISCLAIMER

This report was prepared by students as part of a university course requirement. While considerable effort has been put into the project, it is not the work of licensed engineers and has not undergone the extensive verification that is common in the profession. The information, data, conclusions, and content of this report should not be relied on or utilized without thorough, independent testing and verification. University faculty members may have been associated with this project as advisors, sponsors, or course instructors, but as such they are not responsible for the accuracy of results or conclusions.

EXECUTIVE SUMMARY

This Mechanical Hip Prosthetic project aims to develop an active powered prosthetic hip designed to improve the lives of individuals who have undergone a hip disarticulation amputation. This device will allow users to drastically improve their quality of life by providing a more energy-efficient, stable, and supportive prosthesis. The project began in August 2025, led by a team of four mechanical engineering students. Sponsors Dr. Dante Archangeli and Dr. Reza Razavian guide the team. The main objective is to create a powered prosthesis capable of fully supporting a 90 kg individual during day-to-day activity. The design will include a natural range of motion within the sagittal plane and compatibility with all standard types of prosthetic knees and sockets. To accomplish this, the team has partnered with local prosthetic clinic, Next Step Prosthetics, to gain valuable insights into user needs and functionality.

The current proposed design integrates multiple ideas generated by the team to create a simple and realistic prototype. This device utilizes a standard brushless DC motor to drive hip movement. The device has been refined through a detailed process involving mathematical modeling, SolidWorks design, and MATLAB analysis to create a prosthesis that benefits the user. The design targets motion within the sagittal plane from -20° to 135°, allowing for a replicable flexion and extension of the joint. The goal is for the device to operate for a minimum of 1 hour before needing to recharge. The system will be controlled through a combination of motor controllers and sensors that automatically detect and determine when to lift.

Throughout the academic year, series of mathematical modeling, designing, and prototyping were done to refine and finalize the system. After a process of manufacturing and machining, the final assembly underwent various tests for performance and validation.

The final prototype was fabricated and assembled using machined steel and aluminum structural members, a geared CubeMars actuator system, embedded controls hardware, and standard prosthetic interfaces. Functional testing demonstrated powered joint motion, structural stability, and successful completion of core mobility tasks including static standing and sit-to-stand transitions. The project validates the feasibility of an active hip prosthetic platform and establishes a strong foundation for future clinical and commercial development.

1 Background

Hip disarticulation amputations account for only 1% of all amputees, and yet it is one of the most debilitating. After such strenuous surgery, many individuals lose majority of their mobility and rely on solutions such as crutches, wheelchairs, or use current market available passive external hip prosthetics. As mentioned, there is only a limited range of passive hip joint prosthetics available, typically fashioned as a simple hinge fastened to a socket. However, these current models have been notably difficult to use and maneuver, causing users to expend significantly more energy in compensatory movement in gait. In creating an actively actuated hip joint, users will find more symmetry in gait, and the elimination of excess energy expenditure in mobility. Because powered hip prosthetics are not currently common in the commercial market, successful development of this system may provide a pathway toward improved mobility options for a highly underserved amputee population.

1.2 Project Description

The main goal of this project is to create an active hip prosthetic that allows amputees to experience the freedom of energy-efficient mobility again. Throughout the design process, our team has created and iterated over many various concepts in order to create the most practical solution. Each week, our team meets with our project clients to guide and inform design choices. In addition to our clients, we have also had unique opportunities to work with a local prosthesis clinic, Next Step Prosthetics. This collaborative opportunity has allowed us to speak directly to a hip disarticulation patient, as well as utilizing materials such as genuine lower leg and knee joint prosthetics, and their facility 3D printing. Additionally, in our connection with NextStep Prosthetics has accounted for majority of fundraising through in-kind donations. Following the completion of the NSF I-Corps Aspire Course, we are currently waiting to learn if or when the funding will be available, as it was put on hold due to the previous government shutdown. However, with our allocated initial budget of $4,500 and in-kind donation, our team is still on track to remain within budget. Each of the factors mentioned above are continuously aiding the iterative design process of an active hip prosthesis.

1.3 Deliverables

The primary goal of designing, building, and testing an active powered hip prosthesis is to restore hip motion and eliminate excessive energy expenditure in prosthetic use for individuals who have lost their full leg during hip disarticulation. For this design, the baseline is to have a functional prototype that has active actuation with similar degrees of freedom to a normal leg. This should also be able to be controlled through some sort of control system that the user could control. As this is an upper leg prosthesis just for the hip, it must integrate with a standard prosthetic knee and a standard hip socket. In addition, it would need to be completed by a final report that includes the design specifications, control logic, safety documentation, and recommendations for continued development of the device. Regarding deliverables outside of the device itself, we are responsible for supplying funds outside of the further allocated amount, as well as keeping a detailed bill of materials and budget outlining fiscal aspects of the fabrication process. To assist in keeping us on schedule, a detailed Gantt Chart has been created in which class and client deliverables are included and sorted into various stages of progression. This project is also aiming to be a part of the NIH DEBUT Challenge for rehabilitative and assistive technologies, which includes additional deliverables to be carried out next semester, which could include items such as video demonstration, technical abstract, and supporting documents. The challenge guidelines have not yet been confirmed, which we are anticipating in the spring of 2026.

1.4 Success Metrics

In measuring success for this project, there are many different categories in which we can divide. From a biomechanical standpoint, we measure success in the fluidity and efficiency provided from the design. In other words, how smooth and natural mobility is during use, as well as lifestyle integration factors, such as support and comfortability. Success in controls and electrical fields consists of programmed and intelligent components such as sensors, motor drivers, and electric efficiency and durability. Ensuring that the motor is successfully able to deliver the necessary power at certain times with minimal malfunction is ideally the goal for the active actuation of the design. Furthermore, mechanical success for this design would include gears capable of handling the imposed loads, shafts able to sustain torque transmission, appropriate bearing selections and installations, and structural integrity in the housing and bracket components.

Bringing each of these fields together, the design overall is aiming for active motion in the sagittal plane, a minimum continuous run time of 1 hour, and must be load bearing of an individual up to 90 kg. Further, in material selection and durability, we aim to construct a system that is as light as possible but allows users to comfortably put their weight onto it. We plan to test these by using a bypass method to measure and test the device.

2 Design Requirements

This chapter includes a list of the requirements that the customers have for us as engineers. After the customer requirements were outlined, they were used to give us quantifiable engineering requirements. From those quantifiable requirements, we created a house of quality to best identify areas to prioritize throughout the design process.

2.1 Customer Requirements (CRs)

Our customer is a hip disarticulation patient seeking to regain an active and functional lifestyle beyond what is possible with a passive prosthetic. The design is guided by a set of defined Customer Requirements. These include providing a stable leg capable of supporting a 90 kg user (CR1) and enabling effective walking performance (CR2). The device must also be easy and comfortable to use (CR3) to support daily activities. To ensure practicality, the prosthesis must incorporate efficient battery performance (CR4) and allow for adaptable use with standard prosthetic components and existing hip sockets (CR5). Additionally, the system must assist the user during sit-to-stand transitions (CR6) and stand-to-sit transitions (CR7), improving overall mobility and independence. Together, these requirements define the functional and usability goals of the powered prosthetic hip

2.2 Engineering Requirements (ERs)

To translate these customer needs into measurable design targets, a set of engineering requirements has been established. These are summarized in Table 1:

Table 1: Summary of Engineering Requirements

Requirement	Target
ER 1: Durable	≥ 18 load test cycles
ER 2: Lightweight	< 15 lbs
ER 3: Compact	≤ 14 in length
ER 4: Range of Motion	-20° to 135°
ER 5: Torque	66.2 Nm
ER 6: Cadence	1.25 steps/sec
ER 7: Energy	Within 20% of natural energy used

These metrics served as design gates throughout development; subsystem decisions that failed to support these targets were either redesigned or eliminated.

2.3 House of Quality (HoQ)

Quality Function Deployment

Project title: Horizon Hip
Team Members: Aiden Camisa, Victoria Lyon, Matthew Martinez, Quinn O'Neill
Date: 3/20/2026

Correlation:

+	.	-
Positive	No correlation	Negative

Relationships:

9	7	3	1	0
Strong	Moderate	Intermediate	weak	none

			Desired direction of improvement (↑,0,↓)	0	v	v	^	^	^	^				
		1: low, 7: high	Engineering Requirements (How's) →	Structural integrity with use	Weight of >=15lb	Length of 14 in or less	ROM from -20 ° to 135°	Desired torque of 66.2Nm or greater	Cadence of 1.25 steps/sec or greater	Lasts for 1 hour of regular use	Weighted Score	Competitive evaluation (1: low, 5: high) Satisfaction rating	Helix 3D	Unpowered Hinged Pylon
		Customer importance rating	Customer Requirements - (What's) ↓											
1	7		Support 90kg individual	9	1	0	0	7	0	0	119	5	5	5
2	4		Ability to walk	9	3	0	9	9	9	7	184	5	5	3
3	2		Ease and comfortability	1	9	9	7	0	7	7	80	4	4	2
4	1		Efficient battery life	0	1	0	1	7	3	9	21	3	-	-
5	6		Ensure standard attachment above and below	3	3	3	1	0	0	0	60	5	5	5
6	5		Sit to Stand	9	3	1	9	7	0	1	150	5	3	1
7	3		Stand to Sit	9	3	1	9	7	0	1	87	5	5	5
			Technical importance score	191	80	44	129	148	53	59	701			
			Importance %	27%	11%	6%	18%	21%	8%	8%	100%			
			Priorities rank	**1**	**4**	**7**	**3**	**2**	**6**	**5**				
			Difficulty	4	3	2	3	2	4	1	1: very easy, 7: very difficult			
			Cost and time	5	3	3	2	5	2	3	1: low, 7: high			
			Priority to improve	**2**	**1**	**6**	**4**	**3**	**7**	**5**	1: low, 7: high			

Figure 1: Quality Function Deployment

Compiling each of the identified customer and engineering requirements, the Quality Function Deployment chart depicted in Figure 1 displays the scoring and importance of each interaction. This process prevented subjective decision-making by quantitatively linking customer priorities to engineering effort. As a result, structural integrity was identified as a major area of importance, followed by motor selection and ability.

3 Design Space Research

3.1 Benchmarking

Within the field of powered prosthesis, many different models exist for limbs and joints such as the knee, ankle, shoulder, and wrist. However, there are currently no powered hip prostheses available. Therefore, we selected the most technologically advanced passive hip prosthesis, as well as the baseline, most available model. Further, we include a generic subsystem adapter in our benchmarking process, as our product must be compatible with this system.

The Helix3D Hip Joint by Ottobock [2] is the most advanced system commercially available. Utilizing springs and hydraulics, the system is passively powered by movement and is advertised to create a more even and fluid gait. The system can support up to 100kg and is usable through 130° of motion in the sagittal plane. This system is primarily made up of aluminum components.

Next, the most common type of hip prosthetic available resembles a simple hinge, known as a uniaxial hip prosthetic. While this product is not confined to a specific company, it is a common solution for those who experience hip disarticulation [3]. This model confines motion to the sagittal plane and does not include any kind of passive actuation or mechanism. This system is also able to support 100kg. Additionally, this model is also composed of aluminum.

Lastly, every prosthetic hip joint must have an adapter to connect to a knee joint. It is universally an unofficial standard to implement the use of a pyramid adapter [4]. Able to support up to 181kg and 12N-m of torque, the pyramid adapter is a universal subsystem in the field of prosthetics. The adapter is commonly made of titanium or, occasionally, stainless steel. Our team found it necessary to include this subsystem in our benchmarking to reinforce and ensure that our product will be compatible with the

adapter design.

3.2 Literature Review

Each member of our team independently conducted a Literature Review to gain expertise in various topics spanning prosthetics and biomechanics.

3.2.1 Aiden Camisa

[3] "A normative database of hip and knee joint biomechanics during dynamic tasks using anatomical regression prediction methods" This article talks about the biomechanics of the hip and knee, which will assist in our design by looking at the angles of movement. The authors collected motion capture and force data from healthy adults to establish baseline joint angles, moments, and forces. They used statistical models to predict joint biomechanics based on anatomical parameters. The findings provide standardized data that can serve as a reference for prosthetic design and rehabilitation planning. This database helps clinicians and engineers identify deviations from typical joint mechanics in patients with limb loss or mobility impairments, which can further assist in informing our design.

[4] "GLOBAL STANDARDS FOR PROSTHETICS AND ORTHOTICS" ISO 7206-8: Endurance performance of stemmed femoral components under cyclic loading. This is a page based on the general standards of Prosthetics and Orthotics. It is useful to make sure we follow global standards for devices. This resource guides our team to ensure our prosthetic device meets rigorous performance and safety criteria. It is particularly relevant for hip disarticulation prostheses, where mechanical reliability and alignment are critical.

[3] "Hip biomechanics" This is a page that gives degrees of movement of the hip for all movement angles. The authors highlight how understanding hip mechanics is critical for surgical planning, rehabilitation, and prosthetic design. The paper discusses the kinematics of the hip during various activities, such as walking, running, and jumping. Understanding these biomechanical principles helps optimize gait patterns in amputees, which was identified as a critical aspect by Prosthetist Mentor Mike K.

[5] "Powered ankle-foot prosthesis" An example of a powered ankle prosthetic, we could use different aspects of a design for a different joint for the hip. The paper highlights improvements in energy efficiency and gait symmetry compared to passive prostheses. It also discusses the challenges of designing robust and lightweight actuators suitable for daily use. Further, it also includes the importance of integrating sensors and control systems in a powered prosthetic.

[6] "The Design, Control, and Testing of an Integrated Electrohydrostatic Powered Ankle Prosthesis" Another example of an ankle prosthetic, however, utilizes an integrated electrohydrostatic actuation. The paper highlights the importance of precise torque control and real-time adaptability for gait restoration. The findings provide insight into integrating hydraulic and electronic components in lower-limb prostheses, which we have uncovered is no longer a viable option, as advised by our Sponsor Mentors.

[7] "A review of current state-of-the-art control methods for lower-limb powered prostheses" This is a review of different methods for controlling prostheses, particularly for lower-limb prostheses. The authors discuss the advantages and limitations of each method, focusing on robustness, responsiveness, and energy efficiency. They also highlight human-in-the-loop control strategies that improve gait symmetry and reduce user effort. As our team begins to explore control methods, this provides optimal

introductory information.

[8] “Overview of Hip Disarticulation” A general overview of prostheses for Hip Disarticulation, which we found to be useful for comparing designs and revising work. The author specifically reviews socket designs, suspension methods, and joint mechanisms used in contemporary devices. The paper also discusses challenges faced by amputees, including stability, gait symmetry, and energy expenditure.

[33] “Ground reaction forces at different speeds of human walking and running” This study analyzes how ground reaction forces vary with walking and running speed, providing quantitative data on loading conditions experienced by the human body during gait. The findings are directly relevant to the hip prosthetic design, as they inform expected force ranges and loading cycles that the device must withstand.

[34] “Square Adapter with Pyramid” This source provides specifications for a commercially available prosthetic adapter component, including dimensions, materials, and interface geometry. It was used as a reference for standard prosthetic connection interfaces within the project, ensuring compatibility with existing prosthetic systems. The design informed component geometry and was reflected in CAD modeling, as well as in the selection of standardized mounting.

3.2.2 Victoria Lyon

[9] “Does the new Helix 3D hip joint improve walking of hip disarticulated amputees?” A study on comfort and usability for 3 patients, which we found offers insight for design improvements and preliminary preferences. In this study, participants underwent gait analysis before and after receiving the prosthesis. The study highlights the importance of multidirectional motion in restoring functional gait. It also provides empirical data supporting the effectiveness of innovative hip joint designs.

[10] “A pelvic kinematic approach for calculating hip angles for active hip disarticulation prosthesis control” An in-depth study providing useful information regarding sensors and control systems from the natural body kinematics. Using motion capture and sensor data, the authors developed algorithms to calculate real-time joint angles from pelvic motion. The method enables more accurate control of powered hip joints during swing and stance phases. The findings highlight the importance of integrating kinematic modeling into prosthetic control systems, as opposed to other types of control models.

[11] “Loads in hip disarticulation prostheses during normal daily use” A static assessment of the prosthetic leg and hip was helpful in mathematical modeling and general comprehension. The authors measured forces and moments during walking, sitting, and stair climbing in a cohort of patients. Findings indicate that prosthetic components are subjected to complex, multi-directional loads that must be considered in design. This was also helpful information to keep in mind for material and mechanism selection.

[12] "Design and prototype validation of a laterally mounted powered hip joint prosthesis" A Master's student thesis on a laterally mounted power hip, which opposed the common mounting style to the front of a socket. The authors conducted biomechanical tests to validate the range of motion, joint torque, and gait stability. The paper also highlights challenges in actuator integration and weight distribution, which we hope to learn from and integrate into our design thought process.

[13] "Energy expenditure during walking in amputees after disarticulation of the hip. A microprocessor-controlled swing-phase control knee versus a mechanically-controlled stance phase control knee" This study is centered on comparing active knee prosthetics in standing or walking. The data collected measured oxygen consumption and gait parameters during treadmill walking. Results showed that microprocessor-controlled swing-phase knees significantly reduced energy expenditure and

improved gait efficiency. The study highlights the advantages of integrating smart control technologies into prosthetic limbs, which we again hope to smoothly integrate into our design space as we begin to analyze

[14] "Biomechanical gait analysis for a hip disarticulation prosthesis: power source for the swing phase of a hip disarticulation prosthetic limb" In this study, the authors analyze where the body draws power to propel movement after hip disarticulation. The results are useful for improving gait symmetry and reducing compensatory movements, which we found to be a major component of patient dissatisfaction from our interview with an individual with Hip Disarticulation.

[15] "Design and optimization of a hip disarticulation prosthesis using the remote center of motion mechanism" The improvement of walking motion with a prosthetic utilizing the body's center of motion, which is additionally useful in suspension design choices and passive actuation. The authors modeled joint kinematics to reduce the lateral displacement of the prosthetic limb during walking. Testing from this study indicated smoother swing-phase motion and reduced energy expenditure with a remote center of motion.

[16] "Loading of Hip Measured by Hip Contact Forces at Different Speeds of Walking and Running" This study uses motion capture and musculoskeletal modeling to quantify hip contact forces during walking and running across a range of speeds. The authors found that hip forces rise significantly with increasing speed, and that running produces substantially higher loads than walking. They also show that muscle activity, especially hip adduction and extension moments, is a stronger predictor of hip loading than ground reaction forces alone. The research provides valuable insight into designing exercise programs aimed at stimulating osteogenesis or managing hip joint loading.

[17] "Development of a Powered Four-Bar Prosthetic Hip Joint Prototype" This article describes the design and initial testing of a powered four-bar linkage hip joint using optimization-based design, finite element analysis, and ISO-standard static compression tests. Walking trials with able-bodied participants wearing a prosthesis simulator to test kinematic feasibility were done.

[18] "An Investigation into a Gear-Based Knee Joint Designed for Lower Limb Prosthesis" This paper presents the design of a gear-based knee joint aimed at improving mechanical above-knee prostheses. Using gear design, material selection, and structural testing, the authors evaluate whether the joint can sustain loads typical for gait. They show that the gear-based joint design offers promising mechanical performance, suggesting that such a mechanism could enhance stability or functionality compared to conventional passive prosthetic knees. The work provides a valuable foundation for the trajectory of our current design.

[19] "Comparing the mechanical energetics of walking among individuals with unilateral transfemoral limb loss using socket and osseointegrated prosthetic interfaces" This study compares walking mechanics in eight individuals with unilateral transfemoral amputation before and 24 months after (osseointegrated, bone-anchored) prosthetic interface surgery. The findings highlight that while osseointegration may alter limb-level energetics, it does not necessarily redistribute work within the prosthetic joints; instead, energy losses previously absorbed by the socket may be transferred to the body's center of mass. This work contributes important biomechanical insight into how prosthesis interface type affects gait energetics and may inform prosthesis design or rehabilitation strategies post-osseointegration

3.2.3 Matt Martinez

[20] "Wearable Robotics: Challenges and Opportunities" A book spanning wearable robotics, including exoskeletons and powered prostheses. The author discusses engineering challenges such as

actuation, control, and human-robot interaction. Case studies illustrate applications in rehabilitation and mobility restoration. The book also addresses opportunities for improving energy efficiency and adaptability in robotic devices, which we have taken into account with design and actuation.

[21] AGMA. “Standards & Emerging Technology American Gear Manufacturers Association (AGMA)” A technical standard with important implications, as our design potentially includes the use of a gearbox. The guidelines ensure durability, precision, and reliability, which are crucial for prosthetic joint mechanisms. It includes specifications for materials, load capacity, and tolerances.

[22] “Overview of the Components Used in Active and Passive Lower-Limb Prosthetic Devices” A chapter on the technical details of joints, actuators, and sockets to help guide our selection. The chapter also discusses material selection and design considerations, helping us to further understand integration challenges and trade-offs.

[23] “Total Hip Disarticulation Prosthesis with Suction Socket” A case report that offers practical challenges with sockets, which will help us design a prosthetic that is more socket-adaptable. The study highlights the role of socket fit and suspension in prosthetic performance, which remains relevant in our analysis to determine the best configuration to suspend the joint.

[24] “The biomechanics of trans-femoral amputation” Important and helps to understand load transfer, gait mechanics, and biomechanical limitations in above-the-knee amputations (hip disarticulations). Findings inform alignment, socket design, and joint selection in prostheses, and by understanding mechanical stresses, we can help prevent overuse injuries and improve mobility.

[25] "A multiple-task gait analysis approach: Kinematic, kinetic, and EMG reference data for healthy young and adult subjects A study that provides a baseline for gait and force data on healthy subjects. It supports the design of prostheses that restore natural movement patterns. The dataset is particularly useful for validating powered hip and knee devices. In turn, this can also be used to compare against prosthetic gait data to evaluate function quality.

[26] "State of the Art and Future Directions for Lower Limb Robotic Exoskeletons” Highlights current trends and limitations in robotic exoskeletons, which can inform various aspects of our prosthetic design, such as power, weight, and comfort.

3.2.4 Quinn O’Neill

[27] “EMG Muscle Activation Pattern of Four Lower Extremity Muscles during Stair Climbing, Motor Imagery, and Robot-Assisted Stepping: A Cross-Sectional Study in Healthy Individuals” This study investigates control strategies for powered transfemoral prostheses during stair ascent. The authors designed and tested algorithms that coordinate knee and hip actuation based on real time sensor feedback.

[_28] “On the design evolution of hip implants: A review” Study on hip implants, detailing materials and systems best used to replace a hip. This will allow us a basic idea of how to best connect our prosthetic to the hip of a patient. The findings highlight the growing demand for advanced prosthetic technologies. Understanding population trends supports innovation in high-performance prostheses.

[29] “A novel hip joint prosthesis with uni-directional articulations for reduced wear” The unidirectional hip articulator is the most basic benchmark, as examined in the benchmarking sections.

[30] “Ground reaction forces at different speeds of human walking and running” This paper examines the biomechanics of gait in individuals with and without prosthetic limbs using ground reaction force

analysis. The authors identify characteristic differences in loading, propulsion, and balance between the two groups.

[31] "Shijiazhuang Perfect Prosthetic Manufacture Co., Ltd." The upper-to-lower leg pyramid adapter, a common adapter found on lower limb prosthetics, is a good benchmark for designing the lower attachment for our prosthetic, as mentioned in the benchmark.

[32] "(PDF) A review of gait cycle and its parameters" An analysis of the stages of the walking gait cycle, in which subjects demonstrate how a bionic ankle–foot prosthesis can restore near-normal walking biomechanics. The authors used a powered system comparable to biological muscles. Results showed improved gait symmetry, reduced metabolic cost, and enhanced walking speed.

3.3 Mathematical Modeling

3.3.1 Torque Analysis for Hip Flexion – Matt Martinez

To estimate the torque required for hip flexion, the leg was modeled as a rigid body subjected to gravitational loading and joint geometry constraints. Two equations were used to describe the static torque at the hip:

$$\tau = rFsin\theta \tag{1}$$

Where τ is the joint torque (N·m), F is the applied muscle or actuator force (N), and r is the effective moment arm length (m).

The static torque on the hip was then modeled as:

$$\tau_{hip}(\theta, \beta) = m_{thigh}gr_{thigh}sin\theta + m_{shank}g(L_1 sin\theta + r_{shank}\sin(\theta - \beta)) + m_{foot}g(L_1 sin\theta + L_2 \sin(\theta - \beta)) \tag{2}$$

Where m is the mass (kg), g is gravitational acceleration (9.81 m/s²), L is the length (m), θ is the hip flexion angle (°), β is the knee flexion angle (°), and r is the center of mass (m)

These equations were used to calculate the torque required to lift the leg at various knee flexion angles (0, 60, 90), where the hip angle is 90. The plot shows that static hip torque decreases from 58.3 N·m at 0° knee flexion to 45.8 N·m at 90°. MATLAB was used for data processing and curve generation

3.3.2 Power and Battery Analysis – Aiden Camisa

This analysis outlines the electrical power and battery sizing requirements for an active hip prosthetic. Mathematical modeling using sinusoidal approximations for hip motion and torque interpolations helps to set requirements for the battery. Equations necessary are:

$$\theta(t) = \theta_0 + Asin\left(\frac{2\pi t}{T}\right) \tag{3}$$

$$\omega(t) = \frac{d\theta}{dt} = A \cdot \frac{2\pi}{T}\cos\left(\frac{2\pi t}{T}\right) \tag{4}$$

$$E = \int_0^T \frac{\max(Pmech(t),0)}{\eta_{motor}} dt + P \cdot T \tag{5}$$

Where $\theta(t)$ is the angle with respect to time, θ_0 is the initial angle, $\omega(t)$ is the angular velocity (rad/s), P_{mech} is the mechanical power (W), and E_{step} is the electrical energy per step. The results are in the table below:

Table 2: Battery Sizing for Active Hip Prosthetic

Time (Min)	Battery required (Wh)
10	21.73
20	43.46
30	65.19
45	97.79
60	130.38
90	195.57

3.3.3 *Forces on Leg Due to Walking – Quinn O'Niell*

This analysis provides critical insights into the peak loads experienced by the leg during normal walking. Reaction force is approximately 1.5 times body weight during heel strike/toe-off, and body weight at mid-stance for a 90 kg mass. – Foot length: 24.16 cm, shank length: 39 cm, foot at 90° to shank, heel/toes at 20° to ground. Reaction forces are modeled by:

$$R_1 = 1.5mg \tag{6}$$

$$R_2 = mg \tag{7}$$

R_1 is the reaction force during heel strike and toe-off (N), R_2 is the reaction force at mid-stance (N), m is the mass of the individual (kg), and g is gravitational acceleration (9.81 m/s²). A static equilibrium analysis is then performed to determine force and moment distributions and a geometric modeling of leg segments during gait phases (heel strike, mid-stance, toe-off):

$$\sum F = 0 \tag{8}$$

$$\sum M_k = 0 \tag{9}$$

where ΣF is the sum of forces (N) and ΣM_k is the sum of moments about the knee (Nm).

$$F_t = F_k \sin\theta \tag{10}$$

$$F_a = F_k \cos\theta \tag{11}$$

F_t is the transverse force (N), F_a is the axial force (N), F_k is the force at the knee (N), and θ is the angle

of the force (degrees). - Maximum force: 1.324 kN during heel strike and toe-off

The maximum force of 1.324 kN and moment of 176.65 kNm highlight the need for robust materials and designs capable of withstanding these dynamic loads.

3.3.4 Stress and Strain on a Prosthetic Leg – Victoria Lyon

This is a stress-strain analysis using material properties (Young's modulus), as well as load distribution modeling for standing and walking scenarios, aiding in material selection. Equations used include:

$$\sigma_{axial} = \frac{F}{A} \tag{12}$$

$$\sigma_{bending} = \frac{Mc}{I} \tag{13}$$

$$\varepsilon = \frac{\sigma_{max}}{E} \tag{14}$$

Where σ_{axial} is axial stress (MPa), F is the applied force (N), A is the cross-sectional area (m^2), $\sigma_{bending}$ is bending stress (MPa), M is moment (Nm), c is distance from neutral axis to outer fiber (m), I is moment of inertia (kgm^2), ϵ is strain, σ_{max} is maximum stress (MPa), and E is Young's modulus (MPa).

While standing $\sigma_{axial} = 5.0185$ MPa, $\epsilon = 7.169(10^{-5})$. While walking $\sigma_{axial} = 7.528$ MPa, $\sigma_{bending} = 57.317$ MPa, $\sigma_{max} = 64.845$ MPa, and $\epsilon = 0.0009262$. The stress and strain calculations reveal that walking imposes significantly higher bending stresses compared to standing, with maximum stress reaching 64.845 MPa. This underscores the importance of using high-strength materials like aluminum with appropriate thickness.

3.3.5 Static Force Analysis on Attachments – Aiden Camisa

The static analysis compares various attachment configurations, showing that dual attachments minimize stress concentrations. Static force and moment equilibrium equations are used:

$$F = mg \tag{15}$$

$$M = Fd \tag{16}$$

Where F is the total force (N), m is the mass (kg), g is gravity (9.81 m/s^2), M is the moment (Nm), and d is the distance between bolts (m). Below is the free-body diagram that was used:

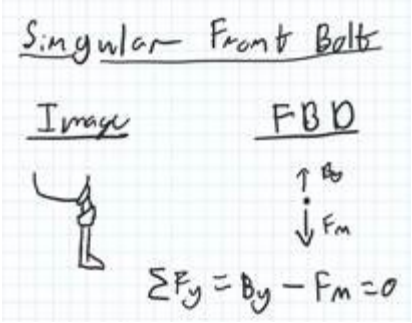

Figure 2: Free-body Diagram of Prosthetic

Then the force is used to find the force per bolt (F_b) and shear stress (σ_{shear}):

$$F_b = \frac{F}{n} \tag{17}$$

$$\sigma_{shear} = \frac{F_b}{A} \tag{18}$$

Shear stress is in MPa, force per bolt is in N, n is the number of bolts, and A is the area (m^2). The table below shows the different attachment used and their respective values.

Table 3: Comparison of Attachment Designs

Type	Force (N)	Moment (N*m)	Force per Bolt (N)	Bearing Stress (MPa)	Shear Stress in the bolt (MPa)
Dual Attachment	882.90	52.974	441.45	13.80	8.78
Laterally Mounted	882.90	70.632	882.90	27.59	17.56
Singular Front Bolt	882.90	88.29	882.90	27.59	17.56
Angled Corner	882.90	105.948	882.90	27.59	17.56

The lowest shear stress of 8.78 MPa in dual setups enhances structural integrity and is optimal for load distribution, reducing failure risk and improving prosthetic stability under body weight loading.

3.3.6 Actuation Static Force Analysis – Quinn O'Neill

This analysis determines the force needed for actuators to achieve a 100° hip motion

range by using moment and force balances for selecting actuators (hydraulic, pneumatic, and electronic linear). The equations that model this are equations (8),(9), (15), and (16). Center of mass (COM) percentages are 43% for the thigh, 43% the shank, and 42% for the foot. The results yield a required actuator force of 142.8 N for a 42.854 Nm moment.

The 142.8 N requirement allows selection from various actuator types, with cost as a deciding factor. All three actuator types (hydraulic, pneumatic, electronic) are viable, but the cheapest reliable option should be chosen for cost-effective design without compromising performance.

3.3.7 Joint and Motor – Matt Martinez

The joint and motor analysis models human hip motion to select appropriate motors and gearing. The torque of the hip is given from a data set, and then body weight (BW) is factored in.

$$\tau_{hip} = -BW \cdot \tau \tag{19}$$

Other variables calculated for the hip joint are angular velocity (ω_{hip}) in rad/s and power (P_{hip}) in watts. θ is the hip angle in degrees.

$$\omega_{hip} = \frac{d\theta}{dt} \tag{20}$$

$$P_{hip} = \tau_{hip} \cdot \omega_{hip} \tag{21}$$

Results were calculated and then modeled using MATLAB. Below are the kinematics at the hip joint during normal gait over one cycle (1.2 seconds):

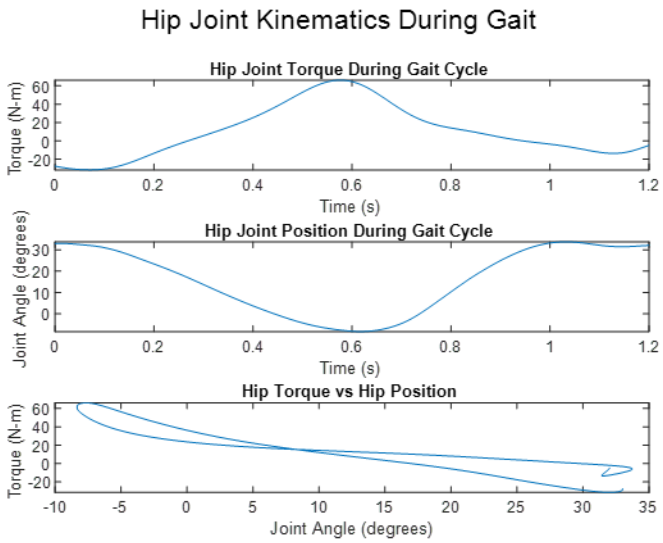

Figure 3: Hip Joint Kinematics During Gait Cycle

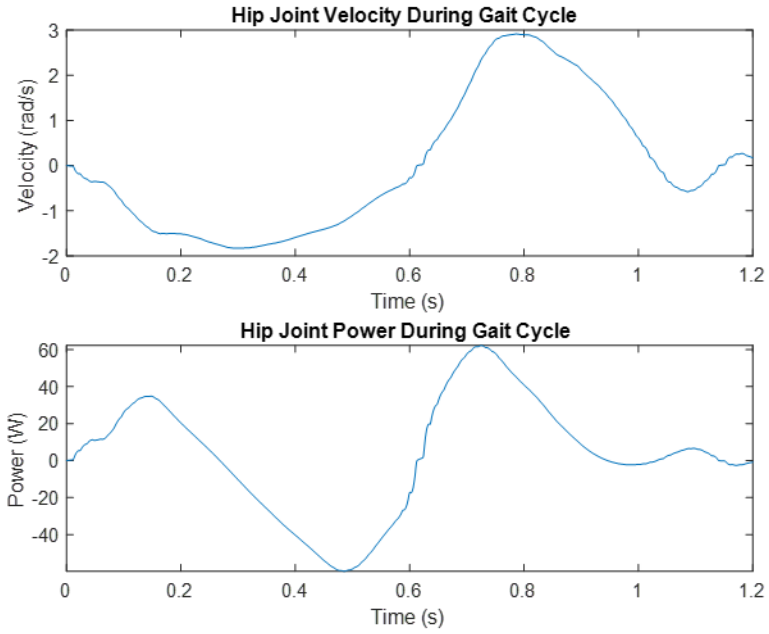

Figure 4: Hip Joint Velocity and Power During Gait Cycle

Next, the specifications from the chosen motor are used to find the current (I) in amps, voltage (V) in volts, and power (P) in watts.

$$I = \frac{\tau_m}{k_t} \tag{22}$$

$$V = IR + k_t \omega_m \tag{23}$$

$$P = V \cdot I \tag{24}$$

τ_m is motor torque (Nm), k_t is the torque constant (Nm/A), R is resistance (Ω), and ω_m is the motor angular velocity (rad/s). The following graphs show these models:

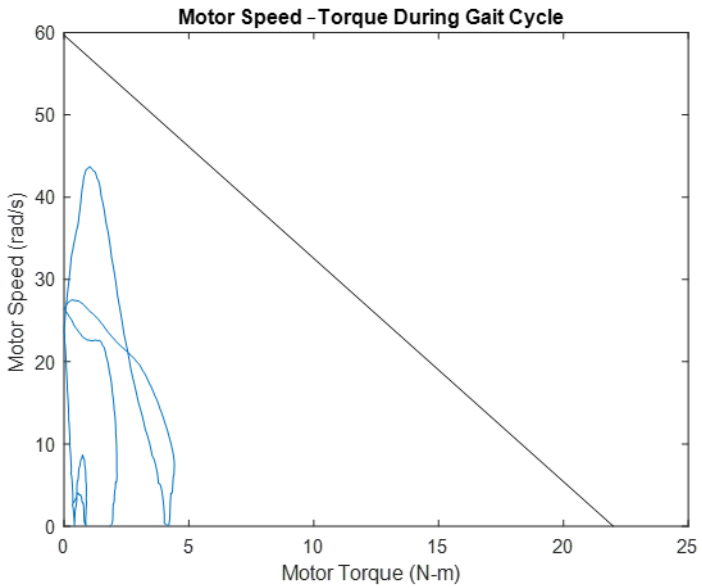

Figure 5: Motor Speed-Torque During Gait

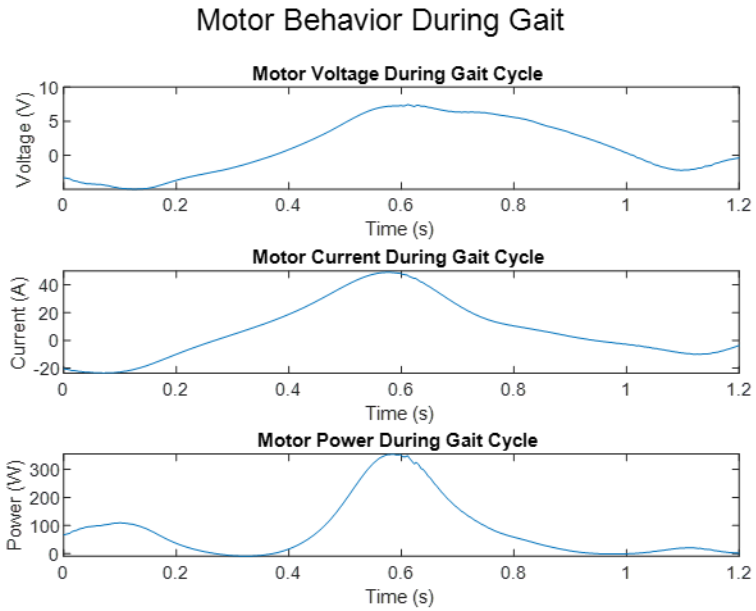

Figure 6: Motor Behavior During Gait

The AK80-9 motor meets torque and power needs, but high gear ratios increase inefficiency.

3.3.8 Preliminary Shaft Material Evaluation – Victoria Lyon

To transmit torque from the motor, a flanged shaft must be mounted directly to the CubeMars motor. Thus, a shaft must be designed to properly transmit oscillations and handle the loads that will be incurred in use. To begin, initial assumptions were defined as:

- $d = 20mm$
- $T_m = 48\ N * m$
- $M_a = 176\ kN * m$
- $S_e(AL) = 270\ MPa \mid S_{ut}(AL) = 110\ MPa$
- $S_e(Ti) = 480\ MPa \mid S_{ut}(Ti) = 550\ MPa$
- $T_a = M_m = 0$

These parameters were then used to compute von Mises stresses of two different materials to check for static failure:

$$\sigma'_a = \sqrt{\left(\frac{32K_f M_a}{\pi d^3}\right)^2 + 3\left(\frac{32K_{fs}T_a}{\pi d^3}\right)^2} \tag{25}$$

$$\sigma'_m = \sqrt{\left(\frac{32K_f M_m}{\pi d^3}\right)^2 + 3\left(\frac{32K_{fs}T_m}{\pi d^3}\right)^2} \tag{26}$$

In which the results are listed in the table below:

Table 4: von Mises Stress Calculations for Potential Shaft Materials

Results	Aluminum (6061)	Titanium (Grade 4)
σ'_a	336.25 MPa	340.71 MPa
σ'_m	.0382 MPa	.0425 MPa
σ'_{max}	336.29 MPa	340.75 MPa

These calculations were not performed solely for documentation; they directly influenced motor selection, shaft sizing, battery sizing, and structural material choices.

4 Design Concepts

This section details the design process throughout the academic year, resulting in the selected components for the final design.

4.1 Functional Decomposition

Table 5: Semester 1 Functional Decomposition Table

Component	1	2	3	4
Actuation	Electronic Linear actuator	Series Elastic Actuators	Rotary Actuator	Variable Stiffness Actuator
Power Transmission	Gear system	Cable	Electrostatic clutch	Belt
Mechanisms	Stewart platform with 2 Links	Ball Joint	Universal Joint	Rigid Links
Suspension / Attachment Configuration	Dual attachment [2 components bolted to the socket]	Lateral [side socket attachment]	Singular front bolt [typical use]	Angled alignment [lower corner attachment,

Table 5 outlines our initial decomposition of applicable items for our design. This served as our main point of reference for major components within the design and further influenced the final selection.

4.2 Concept Generation

Concepts were not individually drawn, but were all understood by each team member.

For means of actuation, we found that the hydraulic was the strongest but most expensive, and the electronic linear actuator was the weakest and cheapest. Therefore, under guidance and recommendation from our clients, rotary robotic motors were a viable option and most accessible for our application. After lots of different research and analysis, our team was able to select a motor that successfully meets and exceeds the necessary force and torque parameters for the prosthetic.

As for power transmission, we opted for a compact and durable system, in which gears were selected and designed for the application. Based on our own experience and knowledge, we felt most confident in designing and selecting a gearset that is capable of handling the variable loading conditions and transmitting the torque effectively.

Lastly, for means of suspension, the lateral side socket is closest to the sagittal center of rotation but is awkward to walk around on as it is loaded to the side of where a sound leg would be. The lower corner would technically be the most structurally-sound for loading the leg when standing but would hinder the range of motion and also be difficult to sit with. Both the front and dual attachments allow for full range of motion in regard to the sagittal plane and further enable ease of installment for professionals.

4.3 Selection Criteria

To evaluate the design concepts, we as a team established criteria that we found would be impactful for our design. This included the performance needs, consistency needs, and practicality of our design. The primary criteria included structural safety, manufacturability, cost of device, and the device reliability and interface. Structural safety was important to make sure that our design could withstand the expected loading while avoiding failure within the device. Manufacturability allows us to consider how feasible the device would be for prototyping, and the final device. The cost of device is important as keeping it available to as many people as possible is important as well. Reliability is important as making sure the device would not fail in critical situations, or under different circumstances will allow us to prevent accidents that could happen within our device. Further, we have learned through the process to additionally evaluate designs based on user experience and practicality, trying to address criteria such as body uniformity (protrusions/ unnatural look and feel).

4.4 Concept Selection

Moving forward to selecting components for comprehensive design, our team decided not to utilize a chart or scoring system but instead participated in an in-depth team-client discussion. This method allowed our team to present thoughts, mathematical analyses, and literature reviews for insight and feedback from our clients, who have experience and expertise in many of the components to be designed.

Our final design decisions were mindful of cost, implementation, and took our client's recommendations into account. To provide power, the CubeMars AK80-64 KV80 motor was selected based on its compact size, rated torque, and gear ratio of 64:1. To actually transmit the motor's power, gears were chosen for their durability, manufacturable advantage, and customizability. Using gears allows our team some room to further change or tweak aspects of the design, such as speed or gear strength. There were no further mechanisms chosen to be used in the design for the sake of simplicity and ease of use and assembly. Lastly, to suspend the hip joint to the socket interface, a single front attachment fastened above the joint was found to be standard within current solutions, but with items such as a lamination plate, the option for dual attachment is available. While not explicitly depicted in concept generation, it is worthwhile to note that many components are to be manufactured from an aluminum alloy that is typically used in prosthetics, while others are to be mild steel materials.

5 Project Management

Our team received an initial investment of $4,500 to fabricate and machine our active hip prosthetic design. So far, we have received many in-kind purchases from our mentors at NextStep, which has been extremely helpful in both application and budget consensus, allowing our team access to genuine prosthetic material and 3D printing technology. A total of $3,127.06 has been spent so far, about 30.5% of the budget. The completed assembly was organized into two main categories: purchasing and manufacturing.

The overall purchasing plan is outlined with each component of the assembly, and the raw material for items to be manufactured.

Table 6: Completed Bill of Materials

Hip Prosthetic Bill of Materials									
Category	**Item No.**	**Description**	**Primary Vendor**	**Unit Price**	**Quantity**	**Make/Buy**	**Manufacturer**	**Lead Time**	**Part Status**
Main Assembly	1	AK80-64 KV80 Motor	CubeMars	$ 911.77	1	Buy	CubeMars		In-Hand
Main Assembly	2	Angular Contact Bearing	BearingsDirect	$ 13.54	3	Buy	NTN Bearings	3-4 Weeks	In-Hand
Main Assembly	3	1030L Gear	Zoro	$ 200.00	1	Buy	Boston Gears	2-3 Weeks	In-Hand
Main Assembly	4	1030R Gear	Zoro	$ 195.00	1	Buy	Boston Gears	2-3 Weeks	In-Hand
Main Assembly	5	Upper Shaft	NAU Machine Shop	$ 7.21	1	Make	Quinn	2 days	In-Hand
Main Assembly	6	Lower Shaft	NAU Machine Shop	$ 7.21	1	Make	Victoria	4 days	In-Hand
Main Assembly	7	Retaining Ring	DSR	$ -	2	Buy	Hillman	1 Week	In-Hand
Main Assembly	8	Shaft Key	Amazon	$ 3.25	2	Buy	dmiotech	3-4 Weeks	In-Hand
Main Assembly	9	Frame (Motor Side)	McMaster-Carr	$ 146.01	1	Buy	Red Rock Manufacturing	3-4 Weeks	In-Hand
Main Assembly	10	Frame (Bearing Side)	McMaster-Carr	$ 131.55	1	Buy	Red Rock Manufacturing	3-4 Weeks	In-Hand
Main Assembly	11	Lamination Plate	NextStep Prosthetics	$ -	1	Buy	Ottobock	5 days	In-Hand
Main Assembly	12	Base Plate	McMaster-Carr	$ 16.02	1	Make	Aiden	3-4 Weeks	In-Hand
Main Assembly	13	Male Pyramid Adapter	Ebay	$ 25.00	1	Buy	Trulife	N/A	In-Hand

Main Assembly	14	Structure Enforcing Bar	NAU Machine Shop	$ 10.17	1	Make	Victoria	3-4 Weeks	In-Hand
Hardware	15	M6-1x25 Socketcap Head Screw	Amazon	$ 19.99	4	Buy	Everbilt	1 Week	In-Hand
Hardware	16	M6-1x15 Socketcap Head Screw	Amazon	$ -	2	Buy	Fgruh	10 days	In-Hand
Hardware	17	M3x12 Socket Cap Head Screw	Amazon	$ -	8	Buy	Fgruh	10 days	In-Hand
Hardware	18	M4x10 Socket Cap Head Screw	Amazon	$ -	6	Buy	Fgruh	10 days	In-Hand
Hardware	19	M8x20mm Countersunk Screw	HomeDepot	$ 2.67	2	Buy	Everbilt		In-Hand
Hardware	20	M6x35 Countersunk Screw	Ebay	$ -	4	Buy	Trulife	10 days	In-Hand
Electronics	21	Adafruit CAN Controller	Adafruit	$ 19.95	1	Buy	Adafruit	2-3 Weeks	In-Hand
Electronics	22	MicroSD Card	Adafruit	$ 13.69	2	Buy	Adafruit	2-3 Weeks	In-Hand
Electronics	23	Buck Converter	Amazon	$ 15.99	1	Buy	YABOANG	1 Week	In-Hand
Electronics	24	Breadboard Jumper Wire	Amazon	$ 10.99	1	Buy	TODOELEC	5 days	In-Hand
Electronics	25	IMU Sensor	Adafruit	$ 6.99	2	Buy	HiLetgo	5 days	In-Hand
Electronics	26	RUBIK Link V2.0	CubeMars	$ 40.00	1	Make	CubeMars		In-Hand
Electronics	27	CAN Bus HAT	Waveshare	$ 39.99	1	Buy	Waveshare		In-Hand
Electronics	28	36V Battery	Amazon	$ 32.83	1	Buy	Amazon		In-Hand
Electronics	29	Battery Adapter	Amazon	$ 5.82	1	Buy	Amazon		In-Hand

For manufacturing processes, the raw material purchased in the table above was either machined by team members or sourced to external providers.

Table 7: Completed Manufacturing Plan

Hip Prosthetic Bill of Materials [MANUFACTURING]											
Category	**Item No.**	**Description**	**Primary Vendor**	**Location**	**Quantity**	**Machinist**	**Process**	**Time Spent (Hrs)**	**Estimated Time**	**Progress %**	**Part Status**
Main Assembly	9	Frame (Motor Side)	McMaster-Carr	NAU Machine Shop	1	Ryan, Red Rock	CNC	1	1	100%	In-Hand
Main Assembly	10	Frame (Bearing Side)	McMaster-Carr	NAU Machine Shop	1	Ryan, Red Rock	CNC	1	1	100%	In-Hand
Main Assembly	12	Base Plate	McMaster-Carr	NAU Machine Shop	1	Matt/Aiden	Mill	5	3	100%	In-Hand
Main Assembly	14	Structure Enforcing Bar	McMaster-Carr	NAU Machine Shop	1	Victoria	Lathe	4	2	100%	In-Hand
Main Assembly	5	Upper Shaft	NAU Machine Shop	NAU Machine Shop	1	Quinn / Aiden	Lathe, Mill	5	3	100%	In-Hand
Main Assembly	6	Lower Shaft	NAU Machine Shop	NAU Machine Shop	1	Victoria / Aiden	Lathe, Mill	7	4	100%	In-Hand
Main Assembly	11	Mounting Bracket	McMaster-Carr	NAU Machine Shop	1	Matt	Mill	5	1	100%	In-Hand
Main Assembly	3	1030L Gear	Zoro	East Valley Precision Machining	1	East Valley	Wire EDM Cutting	1	1	100%	In-Hand
	3	1030L Gear	Zoro	NAU Machine Shop	0	Matt	Mill	1	1	100%	In-Hand

6 Engineering Standards

Design standards play a critical role in both our capstone hip prosthetic project and the broader biomedical industry by ensuring safety, reliability, and consistency in design. For a device that will be used by the human body, adherence to recognized standards, such as those from International Organization for Standardization (ISO) and ASTM International, helps guide material selection, mechanical performance, and testing procedures. In our project, these standards provide a framework that reduces risk of failure, supports ethical engineering practices, and ensures the prosthetic can withstand physiological loads over time. In industry, design standards are essential for regulatory approval, proper use of the device, and maintaining public trust, as they create a common benchmark that all manufacturers must meet. Without them, devices would vary widely in quality and safety, increasing the likelihood of complications for patients and limiting the ability to innovate responsibly.

6.1 Design Standards Research

ISO 10328 - Structural Testing of Lower-Limb Prostheses
This standard defines test methods and load requirements for lower-limb prosthetic components. It was used to understand expected loading conditions and to guide structural design decisions for the hip prosthetic under realistic use scenarios.

ISO 10993 - Biological Evaluation of Medical Devices
This standard provides guidance on biocompatibility testing. It informed material selection decisions to ensure that any components in contact with the user are safe for long-term exposure.

ASTM E8/E8M - Tension Testing of Metallic Materials
This standard outlines procedures for determining mechanical properties such as yield strength and ultimate strength. It was used to validate material properties for shafts, brackets, and load-bearing components.

AGMA 2001 - Fundamental Rating Factors and Calculation Methods for Helical Gear Teeth
This standard provides equations and safety factors for gear design. It was used to ensure gears meet strength and durability requirements under expected loads.

ABMA 9/ABMA 11 - Load Ratings and Fatigue Life for Bearings
These standards define methods for calculating bearing life and load capacity. They were used to select bearings capable of meeting the required lifespan of the prosthetic system.

ISO 68-1/ISO 965 - Metric Thread Standards
These standards define thread geometry, tolerances, and fits for fasteners. They ensured compatibility and proper load transfer in all bolted connections.

ANSI C18 - Portable Rechargeable Battery Standards
This standard defines safety and performance requirements for rechargeable batteries. It was used to guide battery selection and ensure safe operation.

IEC 62133 – Safety Requirements for Secondary Lithium Cells and Batteries

These standard addresses lithium-ion battery safety, including thermal and electrical risks. It was used to ensure safe integration of the battery system.

RoHS Directive (2011/65/EU)
This standard restricts hazardous substances in electronics. It guided component selection to reduce environmental and health risks.

6.2 Design Standards Used

Motor standards
Our motor the Cube mars AK80-64 KV80 follows Ce and RoHS Standards promoting general safety of the device. It is Quality assured under the AS9100D and ISO 17804 standards assuring that it works as intended and promoted. It is rated under Class H insulation, allowing it to withstand up to 180 degrees Celsius. And it uses standardized communication protocols like CAN and UART. These are shown within our bill of materials (BOM) (Table 6) and Testing 9.2.5.

Screws
All the systems screw use mostly ISO metric standards (ISO 68-1 and ISO 965) or UTS standards. Both detailed safety requirements differ in forms of units used for standardization. These will be included in the BOM (Table 6).

Gears
Our gears are ordered from Boston Gears, which follow ASME and AGMA 2001 standards, abiding by standardized sizes for ease of use and safety thresholds. One of the gears is cut to reduce the range of motion to desired size. The gears can be seen in use from the BOM and our range of motion tests is 9.2.4.

Bearings
Our Bearings use ISO standards detailing international safety standards ensuring strong manufacturing quality as well as ABMA standards for standardized bearing sizes and bearing types. These are used in our BOM and out moving tests 9.2.6 onwards.

Bracketing/Shafts
Our aluminum and steel follow ASTM (E8/E8M) internation standards for metal strength and safety, ensuring our materials are of ample quality. The metals will be machined in the NAU machine shop, which follows OSHA standards of safety and EPA environmental safety standards, along with additional codes specific by the shop. These are seen in our 3.3.5, 3.3.6, and 3.3.8 calculations and throughout all our testing and procedures.

Battery
Our battery, the HB Power Li-ion 10S1P2200AA01, uses a variety of different standards. It follows OSHA safety standards ensuring safety to those using the battery. It follows ROHS restrictions of hazardous standards for not using overly dangerous materials. ISO standards for international safety codes. IEC 62133 standards for lithium safety. ANSI C18 standards for safety and performance requirements for specifically portable rechargeable batteries. These are seen in our power usage test 9.2.3 and our BOM.

Control Systems

Our control system uses a Raspberry pi 4b and an Adafruit Feather RP 2040. Both follow the safety standards of ESD electronics safety standards and IoT cybersecurity standards. They both use sizing standards of GPIO pins and I2C, SPI, and UART control standards. The wires use SWG wire gauge standards and ISO international safety standards. Any other standards for the control system are set by the standards of the batter powering it. These are shown in our BOM.

IRB

The Institutional Review Board dictates standards and rules for testing a device like our prosthetic. The group will be completing the readings and training and has submitted the device to the IRB so we are ready to test our device in the safest way possible. These are shown throughout all our tests involving us as participants.

7 Design Validation and Initial Prototyping

7.1 Failure Modes and Effects Analysis (FMEA)

During our design and prototyping of our initial design, we used a Failure Mode and Effects Analysis (FMEA) to identify critical failure points in our design. There were many possible errors that were identified that could cause harm and failure in the leg, however some of the most critical points come from our motor, our shafts and gear trains, and the attachment plate for connecting to the socket at the waist. When looking at the critical point that appears when for the motor it was determined that we felt the motor may just complete its action and not provide sustained torque and power for our system during moments of the gait cycle. To mitigate this issue, we included manual testing as well as keeping a consistent torque loop. This was in the form of hours spent testing, where we controlled the motor to determine the max and minimum positions and set our program to keep the consistent position and torque when not moving. This was beneficial and relatively had low risk trade ffs as this was something that we needed to implement anyways into our code for it to perform our tests. For our critical failure of the motor shafts and gear train we found that some extremely severe issues are either the motor shaft breaking or the motor shaft coming detached or misaligned from the rest of the system. Both possibilities could cause the person to become unable to walk and therefore possible, leading to injury in the event of a fall. To help remedy and to reduce the errors that this happens we used our shafts initially in our prototype and we included spacers where necessary to get them to align properly. This did solve both of our problems as testing on our prototype allowed us to observe no deformations within our shafts and to properly align our gears to ensure a good meshing within our design. Some risk tradeoffs we considered when making this choice, were while we felt confident the motor shafts would not break, we knew that if they did somehow break during prototyping, we would be left without shafts or having to entirely redo our design to create proper space. If the gears and system did not align, this would be a bigger issue, as it could lead to damage to the gears and problems moving if they were not working. Our potential critical failure that had the highest risk priority number was our attachment plate of our design. This is the way that our plate was going to attach to the socket of the individual and how upon multiple uses of the device if it fails and becomes lost within our system. To solve this issue, we performed a maintenance check on our device where we would take five minutes at the start of any test to tighten down any lose screws or systems that fell off. This did include our attachment system which had the two bolts used to connect into the leg. We also performed a standing test to evaluate if our leg could support the weight of the individual and to ensure the leg does not detach from the leg. Finally, our team determined that the risk tradeoff is that minimal as when we perform these tests, we aren’t increasing the inherited risk of using the device.

Table 8: FMEA Identification, Classification, and Action Results

1. Identify					2. Classify				3. Take action				4. Action results				
Item (component, part, assembly)	Function	Requirements	Failure mode	Effect(s) of potential failure	**Severity**	**Classification**	Potential causes of failure	Current design controls (prevention)	**Occurrence likelihood**	Current design controls (detection)	**Effectiveness of best method of detection control**	**RPN (Risk priority no.)**	Recommended action(s)	**Severity**	**Occurrence**	**Detection**	**RPN (Risk priority no.)**
Motor	Providing torque to the shaft	Motor must provide enough torque, smooth, accurate torque/positioning	Control instability or sustained vibration during gait	User discomfort, reduced balance, risk of fall, joint wear	9	Safety	Poor control tuning, insufficient damping	Torque limits, firmware control	3	Manual Testing, Encoder	3	81	Implement rate limits, use high-rate inner current/torque loop	9	2	2	36
Motor	Providing torque to the shaft	Motor must provide enough torque	Motor cannot meet required torque to lift leg	Leg stops moving	4	Product failure	Motor is defunct	Product testing, inspection	1	Torque monitor, current sensing	1	4	Maintenance schedule	5	4	3	60
Motor Shaft	Power Transmission	Transmit movement	Detaches from motor	Hinders rotation	10	Safety	Fastener failure, vibration	Motor casing, using standard bolts	3	Gait stability	4	120	Include repair kit, include fasteners or clamps with design.	10	2	2	40
Motor Shaft	Power Transmission	Handles load	Shaft breaks	Joint & leg detaches	10	Safety	Material failure	Material Selection, mathematical modeling	2	Gait stability	4	80	Replace shaft, bring to prosthetist	5	3	3	45
Battery	Provide Power to the motor	Provides enough power for the motor to allow it to produce the required torque	Does not reach required power	The motor doesn't power the leg, and the leg is not able to reach the required gate	4	Product failure	Dysfunctional battery. Low power battery.	Mathematically determines the amount of power required for the motor	1	Low voltage alarm in testing	1	4	Use battery with 20-30% capacity margin	5	4	3	60
Battery	Provide Power to the motor	Provides enough power for the motor to allow it to produce the required torque	Wires break / detach from motor	Leg stops moving with power. potential danger with loose wires	6	Safety	wires not secured tightly	Clips built into motor, and no major movement of motor or battery, and sealing of the wires to the mold	3	Motor stops working, look at wire	2	36	secure wires closely to the mold to prevent damage and movement	7	3	2	36
Raspberry Pi Controller (Electrical system)	Acts as a computer to provide control	Simple and easy Interface	No Control of leg	Locks in place or becomes frozen in place. Possible tripping and injury	4	Product failure	Code is wrong or something is unplugged	Raspberry pie with a CAN bus attachment to the motor.	4	Testing the code and wiring before using it on a individual	5	80	Implement a test sequence to make sure everything works.	4	4	1	16

Attachment Plate	Suspend system on socket	Securely hold system without movement	Detaches from socket	System detaches	10	Safety	Extreme wear, unforeseen force	Secure standard fasteners	2	Stability, inspection	3	60	Safety test, user manual	5	4	3	60

The highest-risk failure modes were associated with sudden loss of structural support, shaft detachment, and unstable controls behavior. Mitigation efforts therefore prioritized redundant fastening methods, conservative shaft sizing, torque limiting, and pre-use verification procedures.

7.2 Initial Prototyping

Initial prototypes intentionally prioritized rapid learning over aesthetics, enabling the team to identify packaging conflicts, alignment issues, and assembly inefficiencies before final fabrication.

While designing and building our initial prototype, our team had been prioritizing simplification of the system, applying our current knowledge to the best of our abilities. Our first design iteration featured a large housing box, single shaft, bearing, and T-shaped adapter, as depicted in Figure 7 below:

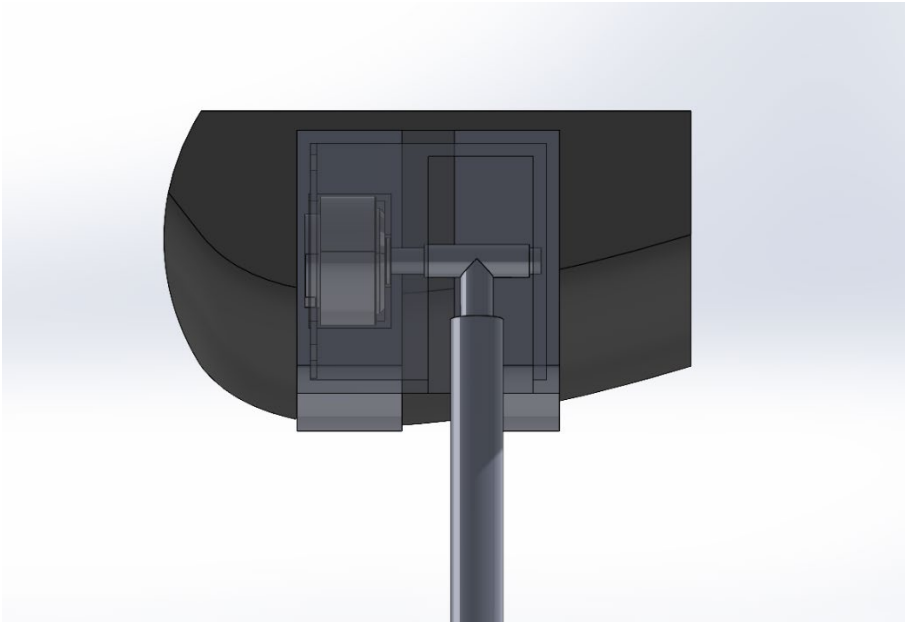

Figure 7: Initial Prototype Design

Further analysis of this design allowed us to take similar concepts and rework items that were no longer feasible, in which the following questions were answered:

What question are you trying to answer with the prototype?

With this design, our team was aiming to answer:

- Is this design practical and intuitive?
- Does this design facilitate movement in the sagittal plane?
- Is this design actively actuated?
- Is this manufacturable and user friendly?

What was the answer?

Building the physical prototype was extremely informative to our understanding and application, which revealed in various aspects what concepts worked, and what concepts needed to be redesigned. We found each question to be answered:

- Simple function does not imply practical function.
- The design is not intuitive or desirable, the system housing is extremely bulky and would protrude awkwardly for users.
- Movement is facilitated in the sagittal plane, but rotation is extremely far removed from the accurate hip center of rotation.
- The design is hard to assemble and manufacture, the housing is completely closed off except for the pylon clearance slot, which does not allow for components such as the motor to be assembled within it.

How did it inform design/how do you plan to iterate based on this new info?

Following the completion of this prototype design, our team collectively decided to reconsider the design for the prosthetic. In doing so, we adjusted design priorities, such as ease of assembly and user-friendly integration. Additionally, taking factors such as center of rotation closeness and weight distribution in account as well helped to inform us of how to move forward in the iterative design process and start of our redesign.

7.3 Re-design

Using our initial prototyping results, we found multiple possible problems within our design. To address these issues, we decided to review and then redesign parts of our prosthetics. Our new design uses a gear-based drive train with the motor attached at the leg that rotates around the center of rotation of the mechanism. Seen in figure 8 below, we can see that we use two spur gears powered along their respective shots and held together with a gear bearing combo. We proceeded forth, doing our calculations based on this design as we felt we would lean more towards this than our old design.

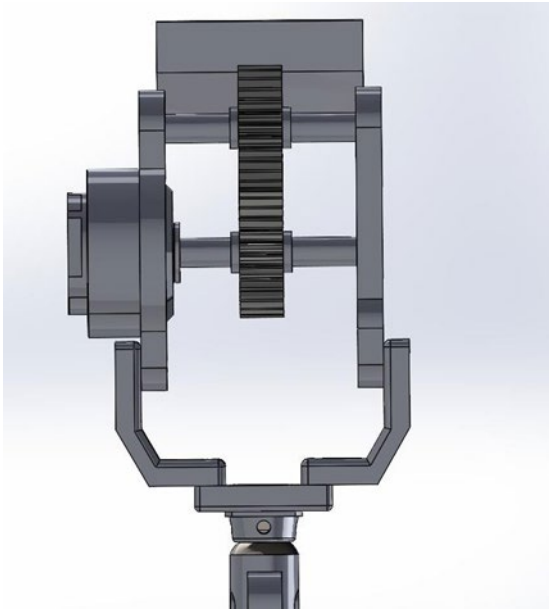

Figure 8: Current Prosthesis Design

7.4 Additional Engineering Calculations

7.4.1 Structural Frame Analysis – Aiden Camisa

For structural frame analysis, I performed a stress calculation based on frames bearing wall thickness. In addition, I looked at the factor of safety of a variation of the lower bracket designs. Finally I confirmed everything by using a finite element analysis within SolidWorks on our models to test the stress and strength. Some of the assumptions we used for this calculation is that the body weight would be a 882.9N, with a reaction force of 1324 N. In addition, we would have a torsional motion of 120 N*m for the short-term movements within the motor itself on objects. In addition to these values, I used constants from aluminum 6061 T-1 and the sizing of our 3D model.

To perform these calculations, I used the equations below to allow for my calculations. In addition to the variables above, I used the thickness, lengths of certain pieces, and as well as diameters of the inside and outside frame portions around the bearings.

$$\sigma = \frac{M}{I} \tag{27}$$

$$M = F \cdot L \tag{28}$$

$$I_{lower\ frame} = \frac{bt^3}{12} \tag{29}$$

$$I_D = \frac{\pi(D_0 - D_i)}{64} \tag{30}$$

$$FOS = \frac{\sigma_y}{\sigma} \tag{31}$$

Using these equations, I am able to calculate the FOS for the bearings of 3.24 which is above our

minimum of 2. This shows that the thickness of frames around the bearings will hold during stress. In addition to this I get a stress value of a newer design to only be 42.55MPa which is lower than our old design. This shows that while both beat the aluminum yield strength, the new design beats it by a significant margin compared to our old design. Finally, to help verify this info, I used simulation software to look at the stress within the system.

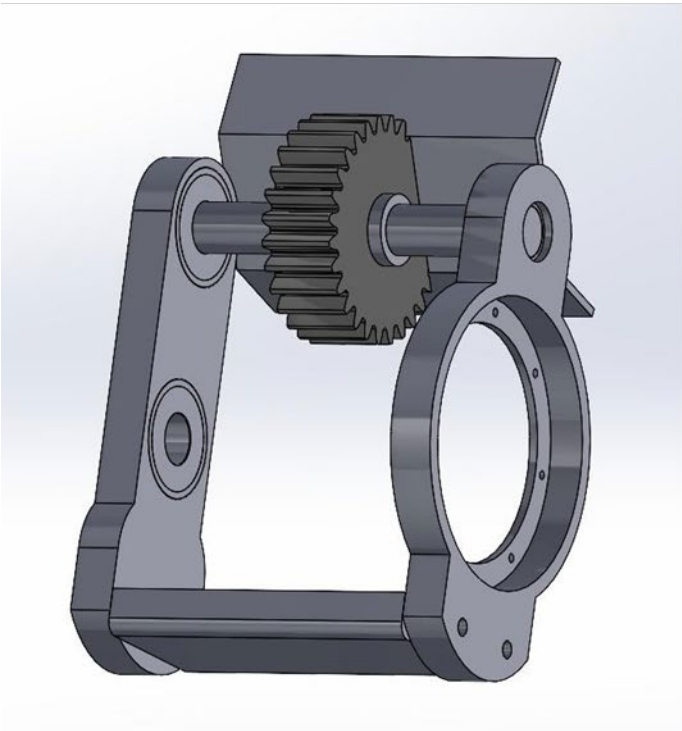

Figure 9: New Frame design Model

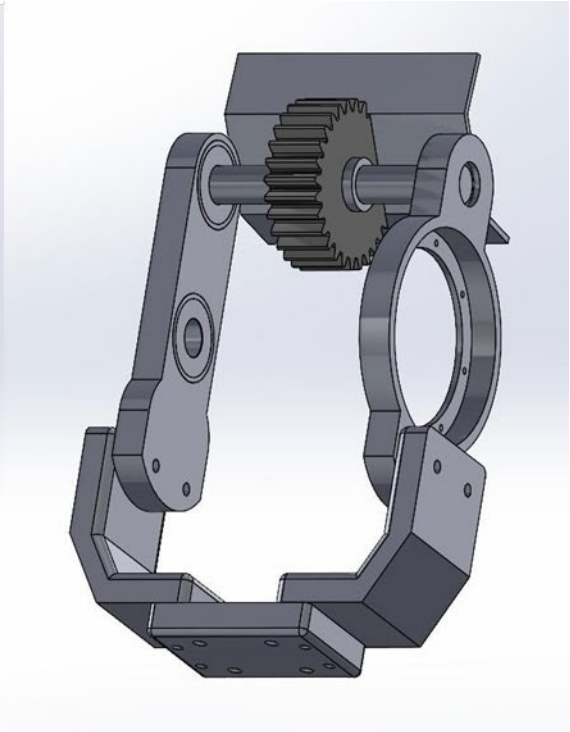

Figure 10: Current Frame design Model

Above we can see the current revisions of the frame with our potential new frame on the left and a older design on the right.

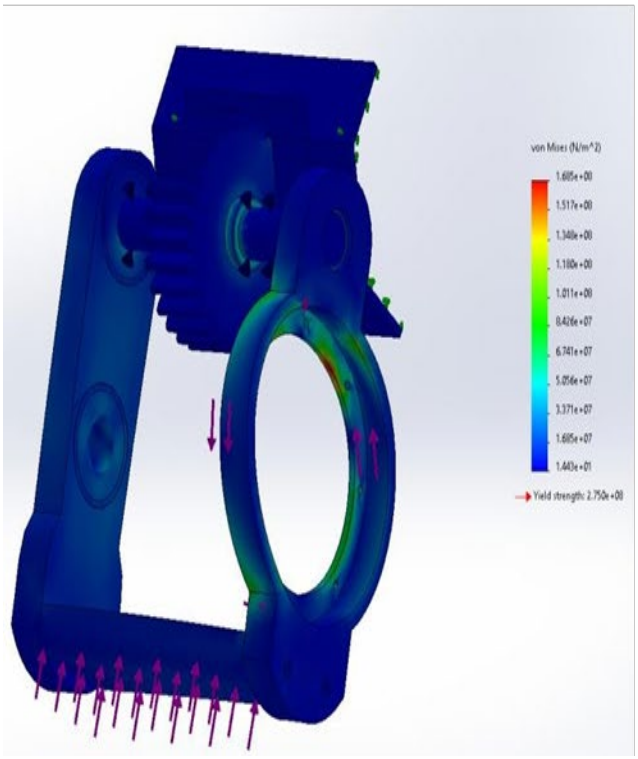

Figure 11: Stress for New design

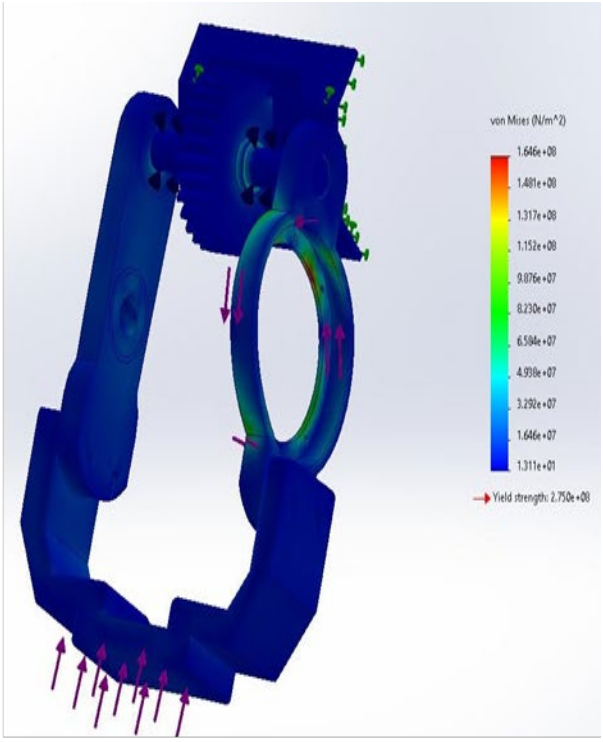

Figure 12: Stress for Current design

Above we can see just the stress variations of the SolidWorks simulation. A couple of interesting things about these models is some of the increased load caused by the motor on the lower shaft on our old design with the newer design, we can see that it disappears. In addition to this we can see that the values are relatively small, showing that while there is difference the forces are not massive enough to cause great breaks within our system. Overall, we can see that the newer flatter design appears to work better so we will be proceeding forth with this design.

7.4.2 Battery Analysis – Quinn O'Neill

The team needs a battery to power the motor in order to lift the leg. This battery must be chosen based on if it allows the motor to produce enough power, and the energy stored by the battery is enough to allow the user to use the leg for long enough.

To start, we need to find the required voltage of the motor. To do this we found the required torque and rotational speed of the motor based on a study and dataset detailing the amount of torque at the hip for lifting the leg, and the rotational speed at which it is lifted [28]. Using the formula:

$$P = T \times \omega \tag{32}$$

Where P is power (Watts) T is torque (Nm) and ω is rotation speed (rad/s). Plugging the data and formula into MATLAB we got a graph that looks like this:

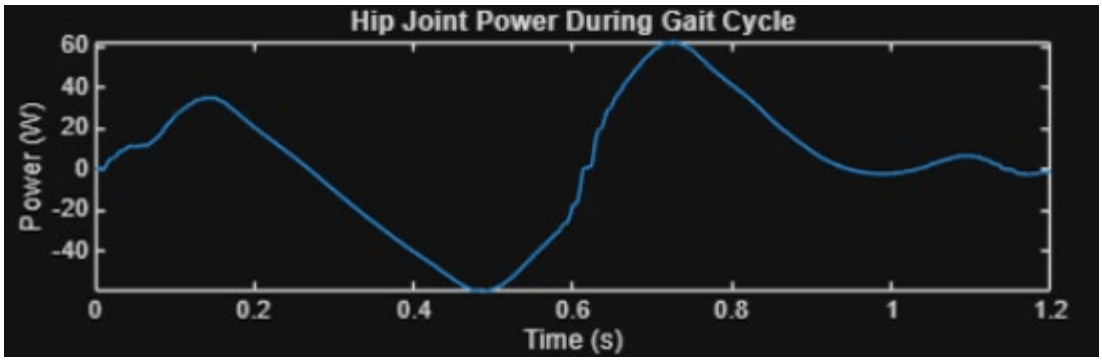

Figure 13: Hip joint power per gait time

From this data we get an average of 23.98 Watts per step. Then using listed data from our selected motor, the Cubemars AK8064 KV 80, we were able to find the required amperage per the gait cycle using this formula:

$$I = T/kt \tag{33}$$

Where I is current (Amps), T is torque (Nm), kt is a rated torque constant (Nm/A). resulting in following:

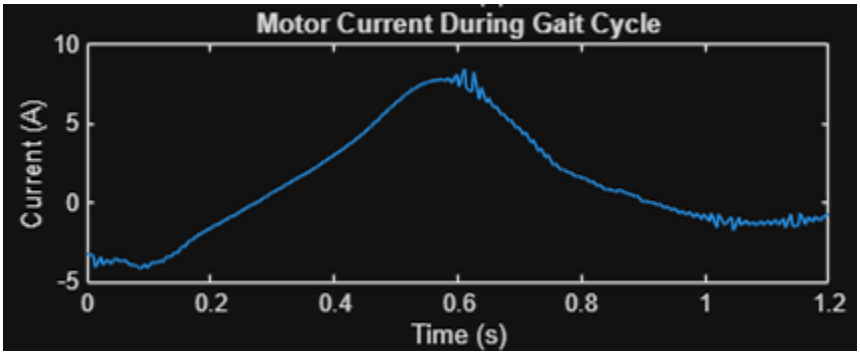

Figure 14: Motor current per gait time

Then doing a matrix division of the Power and the current results in the following graph, showing the voltage for the motor required.

$$V = P/I \tag{34}$$

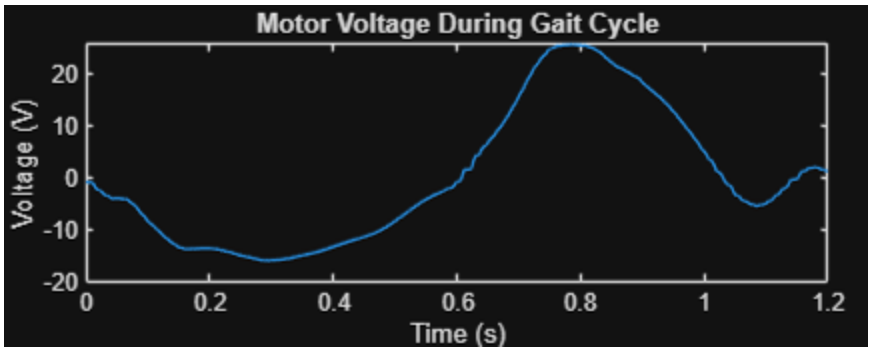

Figure 15: Motor Voltage per gait time

This graph gave us the Maximum motor voltage value of 25.7503 Volts. The motor is rated for Voltages of 12/24/36/48, meaning the minimum required input voltage for this to motor to function at its max efficiency is 36V.

Our next goal is to find how much energy we need for the users of our product to achieve what they want to and then find a battery with that Energy. First, we need to set a limit to our user's goal. We decided we wanted to allow our customers the recommended 10,000 steps a day for general fitness. Because we are only designing for 1 leg, we need to allow only 5000 per that leg, however since we want to allow our user to go above and beyond, and account for activity other than walking, we landed on an allowed 10,000 steps for our leg.

Taking the average power per step of 23.98 Watts and taking an average step time of 1.2s from our walking study [], we can determine the Energy used per step with the following formula:

$$E = P * t \tag{35}$$

Where E is energy (Joules) and t is time (seconds), resulting in a step energy of 28.78 J. Multiplying by our desired step count of 10,000 we get a required energy of 287,800 Joules stored within the battery. Most batteries have a listed number of Amp-hours or Watt-hours. Watt hours are a form of energy stored in a battery per full charge. Amp-hours can easily be converted to Watt-hours by multiplying our chosen battery voltage. Converting our Energy to Watt hours requires the following conversion formula:

$$E(Wh) = \frac{E(j)}{60\left(\frac{min}{hr}\right) \times 60\left(\frac{s}{min}\right)} \tag{36}$$

Resulting in a required battery rating of 79.9 Wh or 2.22 Ah

From the required energy and voltage, the team searched for and was able to find a battery that met these requirements and a relatively lightweight compared to other 36 V batteries on the market

Figure 16: Selected battery for the team

The selected battery has a rated voltage of 36V, capacitance of 4.4 Ah, and while this battery unfortunately has no listed weight, it has a listed dimensioning of $1.3 * 3.5 * 5.3\ in3$, significantly smaller than many 36 V batteries on the market.

7.4.3 Shaft and Bearing Analysis - Victoria

Building further upon previous shaft analysis, the updated design features two shafts that must support the gears, bearings, and properly transmit the required torque to enable hip rotation. Additionally, to assist in handling the load imposed by use, bearings will be utilized. To begin preliminary shaft design and bearing selection, it is necessary to note how the gears and bearings will be installed onto the shaft—the bottom shaft of the design is directly mounted to the motor and is fitted with a single bearing on the opposite side in which the inner ring will be rotating. However, the upper shaft features bearings on both sides, and is to remain stationary, therefore the upper shaft bearings outer rings will rotate. As a result, a tight interference fit will be used to install the bearings to the shafts. The top shaft will require a tight inner ring, with a loose outer ring as the load rotates with it. Oppositely, the bottom shaft bearing will require a tight outer ring fit and loose inner ring fit. The interference for these installation types will be computed further in fabrication processes.

For shaft materials, it is recommended to use low carbon steel. With this in mind, a preliminary material of AISI 1050 CD is selected for both shafts. The steel has the following material properties:

$$S_{ut} = 690\ MPa$$
$$S_y = 580\ MPa$$

To determine the minimum diameter applicable, the following assumptions and parameters are

defined:

- $90\ kg$ individual
- Due to oscillating movement in use, the bending stress is completely reversed.
  - $M_m = 0 = T_a$
- Gear face width, $F = 25.4\ mm$
- Shaft length, $L = 115\ mm$
- Maximum moment at the hip joint during flexion, $M_a = 98\ N * m$
- Maximum torque at the hip joint during gait, $T_m = 66\ N * m$, calculated in previous team analysis.
- Initial ratios of $\frac{D}{d} = 1.5$, $\frac{r}{d} = .02$ in regard to the variable diameter sizes and shoulder filets.
  - $K_f = K_t = 2.7$
  - $K_{fs} = K_{ts} = 2.2$
- Initial factor of safety, $n = 1$
- Desired reliability, $R = 0.99$

Note that many of these parameters are preliminary and will require further iteration with solidified dimensioning as a result of gear and bearing selections. To solve for the diameter size, the von Mises stress equation is rearranged:

$$d = \left(\frac{16n}{\pi}\left\{\frac{1}{S_e}\left[4\left(K_f M_a\right)^2\right]^{\frac{1}{2}} + \frac{1}{S_{ut}}\left[3\left(K_{fs} T_m\right)^2\right]^{\frac{1}{2}}\right\}\right)^{\frac{1}{3}} \quad (37)$$

Using these initial values, a diameter of $d = 23.14\ mm$ is computed, which is larger than the required shaft restriction. Further, based upon this result, the center diameter would measure $D = 34.71\ mm$, and notch radius of $r = 0.4628\ mm$. However, as a preliminary calculation, further iteration will be carried out in order to further reduce the diameter size as the dimension ratios were assumed to be worst case, as recommended in *Shigley's Mechanical Engineering Design.* To do so, we now compute actual K_f and K_{fs} values using the radius, and continue diameter iteration.

$$K_f = 1 + \frac{K_t - 1}{1 + \sqrt{a}/r} \quad (38)$$

$$K_{fs} = 1 + \frac{K_{ts} - 1}{1 + \sqrt{a}/r} \quad (39)$$

Where $\sqrt{a}$ is the Neuber constant based on material properties, defined for both bending and torsion:

$$\sqrt{a}_{bending} = 0.246 - 3.08(10^{-3}) \times S_{ut} + 1.51(10^{-5}) \times {S_{ut}}^2 - 2.67(10^{-8}) \times {S_{ut}}^3 \quad (40)$$

$$\sqrt{a}_{torsion} = 0.190 - 2.51(10^{-3}) \times S_{ut} + 1.35(10^{-5}) \times {S_{ut}}^2 - 2.67(10^{-8}) \times {S_{ut}}^3 \quad (41)$$

The updated values are input into a MATLAB iterative loop, computing the diameter until convergence. Note that the converged diameter is still for initial ratios of $\frac{D}{d} = 1.5$ and $\frac{r}{d} = .02$, therefore the stress concentration factors remain as $K_t = 2.7$ and $K_{ts} = 2.2$. Future calculations can provide further accuracy and improved dimensions.

The final converged result yields a diameter of $d = 15.76\ mm$, leaving about $1.24\ mm$ until the maximum diameter restriction is reached. Therefore, the center diameter is $D = 23.64\ mm$, and notch radius $r = 0.3152\ mm$.

Based upon typical human gait, the team previously computed that the leg experiences about $1324\ N$ in ground-reaction forces, composed of $1244\ N$ which is radial, and $453\ N$ which is axial. Accounting for forces in both directions, an angular contact ball bearing will be selected. Using the computed shaft diameter as a guideline for bore specifications, we select an SKF 7202 BE angular contact ball bearing to support each shaft. This bearing has a dynamic load rating of $C_{10} = 39.3\ kN$ and static load rating of

$C_0 = 21.4\ kN$, which is more than suffice for the current application forces.

Further, the shaft will require retaining rings by means of gear alignment, and a key and keyway in order to properly transmit the torque from the motor to the gear set. Given that the minimum center diameter is $D = 23.64\ mm$, we increase to $D = 25\ mm$ and select retaining ring DSR-25. This specific ring is external and thus housed directly on the shaft. This requires a groove diameter of $D_g = 23.9\ mm$, which allows for tolerance from the calculated minimum central diameter. The ring has load handling capabilities of $P_r = 45\ kN$ of thrust on the ring, and $P_g = 8.30\ kN$ of thrust on the groove, which is more than sufficient to withstand the defined thrust experienced in gait. Lastly, in designing a key for each shaft, *Shigley's Mechanical Engineering Design* includes a table in which typical shaft diameters and suitable key and keyway sizes are listed. Considering that this key will sit on the top center diameter, the table is assessed for a $25\ mm$ diameter shaft. A key of $w = 6.35\ mm$ and $h = 4.76\ mm$ and keyway depth of $2.38\ mm$ would be suitable for the shaft.

7.4.4 Gear Analysis - Matt

To support the ongoing development of the powered hip prosthesis, a detailed analysis of potential gearsets for the actuator assembly. The goal was to replace the placeholder gears in the current CAD model with components that are mathematically justified, meet torque and power requirements, and minimize size while maximizing delivered torque. The new gearset must reliably transmit the peak torques observed during gait, operate with low noise/vibration, and fit the spatial constraints imposed by the motor and socket.

To establish constraints, the team assumed that the gear bore must be 0.75 in to accommodate the CubeMars AK80-64 motor shaft and fastener arrangement. Because the design uses parallel shafting, helical gears, if chosen, must be paired as left-hand and right-hand variants. The powered joint must safely transmit 66.2 N-m (585.92 lb-in) of torque, 0.084 horsepower, and rotational speeds up to 27.7 rpm during gait. MATLAB derived joint profiles Figures 3 and 4 showed gait to be the most demanding motion condition. A service factor of 1.25 was applied to account for uniform-to-moderate shock loading, increasing the minimum allowable transmitted torque to 732.4 lb-in.

Using equations and rating methods provided in Boston Gears' *Rotary Drive Products* catalog, the team evaluated spur gears at 14.5° and 20° pressure angles as well as helical gears at 14.5°. Catalog data for allowable torque, horsepower, diametral pitch, face width, and pitch diameter were used to compute gear volumes. Torque-per-volume (T/V) served as the key metric because minimizing component size while maximizing torque capacity is critical for packaging inside a prosthetic hip. Hardened steel gears were selected as the baseline material due to superior load capacity and favorable strength-to-weight characteristics compared to bronze and cast iron. The equations used by Boston Gears are:

$$W = \frac{SFY}{P}\left(\frac{600}{600+V}\right) \tag{42}$$

$$T = \frac{W \times D}{2} \tag{43}$$

$$HP = \frac{WV}{33000} \tag{44}$$

Where allowable torque is T, power is HP, and allowable load is W. Also, SF is the safety factor, Y is

tooth form factor, P is diametral pitch, V is the pitch line velocity, and D is diameter. Equation 42 is for a spur gear. To calculate allowable load of a helical gear, diametral pitch is replaced with normal diametral pitch. Tooth form factors are based on number of teeth and are shown in the tables below:

Table 9: Y Factor for Spur Gears

Number of Teeth	14-1/2° Full Depth Involute	20° Full Depth Involute
10	0.176	0.201
11	0.192	0.226
12	0.210	0.245
13	0.223	0.264
14	0.236	0.276
15	0.245	0.289
16	0.255	0.295
17	0.264	0.302
18	0.270	0.308
19	0.277	0.314
20	0.283	0.320
22	0.292	0.330
24	0.302	0.337
26	0.308	0.344
28	0.314	0.352
30	0.318	0.358
32	0.322	0.364
34	0.325	0.370
36	0.329	0.377
38	0.332	0.383
40	0.336	0.389
45	0.340	0.399
50	0.346	0.408
55	0.352	0.415
60	0.355	0.421
65	0.358	0.425
70	0.360	0.429
75	0.361	0.433
80	0.363	0.436
90	0.366	0.442
100	0.368	0.446
150	0.375	0.458
200	0.378	0.463
300	0.382	0.471
Rack	0.390	0.484

Table 10: Y Factor for Helical Gears

FOR 14-1/2°PA–45° HELIX ANGLE GEAR			
No. of Teeth	Factor Y	No. of Teeth	Factor Y
8	.295	25	.361
9	.305	30	.364
10	.314	32	.365
12	.327	36	.367
15	.339	40	.370
16	.342	48	.372
18	.345	50	.373
20	.352	60	.374
24	.358	72	.377

Across all evaluated gearsets, the helical gears with 10 teeth in Table 13 produced the highest torque per unit volume. Two variants existed with face widths of 1.0 in and 1.25 in. The 1.25-in-wide option provides increased load capacity (948 lb-in allowable torque), comfortably above the 732.4 lb-in

requirement with service factor applied. These gears also meet the 0.75-in bore requirement and have a compact 1.667-in pitch diameter suitable for integration in the hip assembly.

Table 11: Spur Gear Specifications with Pressure Angle of 14.5

Teeth	Power (HP)	Torque (lb-in)	P (Teeth/in)	Face Width (in)	Diameter (in)	Volume (in^3)	Torque per Unit Volume (T/V)
25	.29	742	10	1	2.5	4.91	151.12
11	.38	946	6	1.5	1.83	3.95	239.49
16	.31	778	8	1.25	2	3.93	197.96

Table 12: Spur Gear Specifications with Pressure Angle of 20

Teeth	Power (HP)	Torque (lb-in)	P (Teeth/in)	Face Width (in)	Diameter (in)	Volume (in^3)	Torque per Unit Volume (T/V)
64	.31	779	16	.75	4	9.42	82.7
36	.37	928	12	1	3	7.07	131.26
20	.31	784	10	1.25	2	3.93	199.49
14	.35	890	8	1.5	1.75	3.61	246.54

Table 13: Helical Gear Specifications with Pressure Angle of 14.5

Teeth	Power (HP)	Torque (lb-in)	P – Normal P (Teeth/in)	Face Width (in)	Diameter (in)	Volume (in^3)	Torque per Unit Volume (T/V)
30	.32	818	10 – 14.14	.875	3	6.19	132.15
24	.34	862	8 – 11.31	.75	3	5.3	162.64
16	.29	740	8 – 11.31	1	2	3.14	235.67
10	.3	758	6 – 8.48	1	1.67	2.19	346.12
10	.38	948	6 – 8.48	1.25	1.67	2.74	345.99

The selected gears correspond to Boston Gear part numbers H610R-18004 (right-hand) and H610L-18006 (left-hand). However, as these are minimum capable gears, due to our design height from the CubeMars motor, gears with an increased pitch diameter are necessary. Thus, the H1030 R and H1030L Boston Gear parts are purchased for appropriate design fittings.

8 Final Hardware

Chapter 8 details visuals of the completed assembly and CAD model. Additional component designs necessary for testing, such as a hip bypass and weight testing apparatus, are also shown.

8.1 Completed Assembly

After manufacturing has been completed, the final assembly was put together and prepped for testing. The figures below depict the final CAD model completed and the actual assembly:

Figure 17: Final Assembly

All structural components are manufactured from 6061 aluminum, such as both frames, the connecting bar across the middle, and lower base plate. The two shafts and attaching gear bracket are made from 1081 steel for increased durability. Fasteners visible past the base plate are in place for securing a system cover, in which the cover slides over the exposed fasteners, and a nut is used to hold it in place. The fasteners visible atop the gear bracket are in place for attachement to prosthetic socket interfaces, such as a a lamination plate.

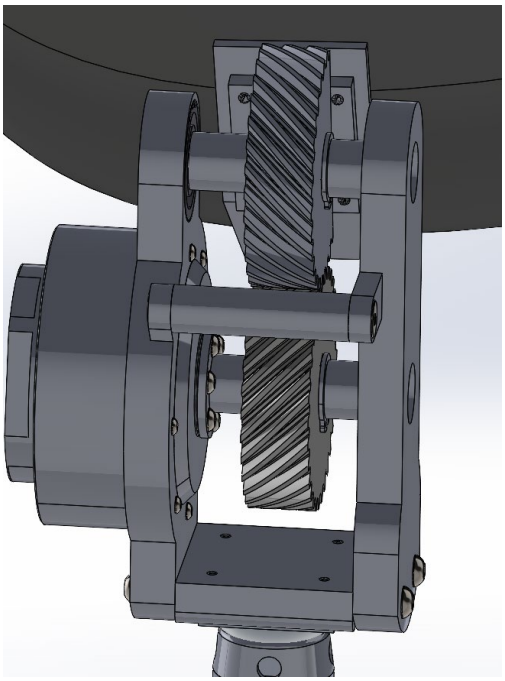

Figure 18: Final CAD Model

8.2 Testing Setup & Hardware

For both bench and functional tests, additional material and setup hardware were necessary. Bench testing refers to any testing of the device while it is not worn and fixed in place, whereas functional testing is any time that the system is worn for activity and motion test.

To fix the system in place, it was mounted to a pegboard tile that was threaded via lamination plate and suspended over the edge of the table. 4 quarter inch fasteners were used to secure the lamination plate and adjoined system to the table.

Figure 19: Bench Test Setup

For functional tests, a separate bypass had to be constructed for individuals with both sound legs to test the hip joint. To do this, the sound leg and lip must be immobilized so that during testing the user is not able to use their sound leg or hip for assistance but must rely on the prosthetic instead. A structure enforcing hip brace and hands-free crutch were combined to adequately suspend the sound leg and restrict the hip.

Figure 20: Hip Immobilizing Bypass

Figure 21: Complete Functional Testing Setup

Figure 22: System Cover

To prevent pinching or crushing, a simple cover was designed and 3D printed to cover the lower-half of the design, which easily slid into the current assembly.

9 Testing

Testing plan references CRs and ERs - which are updated. Top-level summary of testing plan is described thoroughly. Testing procedures are referenced and then summarized in the appendix. Testing results are summarized within a specification sheet describing how ERs/CRs were met or not.

9.1 Top Level Testing Summary Table

Table 14: Top Level Testing Summary

Experiment/Test	Relevant DRs	Testing Equipment Needed	Other Resources
Exp 1 – Device Weight Check	**ER2** – Less than 15 lb	Scale	
Exp 2 – Attachment Verification	**CR5** - Ensure standard attachment above and below	Lamination plate, Female pyramid adapter	
Exp 3 – Power Usage Test	**CR4** – Battery should last throughout the day **ER 7** - Last 1 hour of use	Multimeter/Power supply Weights Mounting System Camera	Arc Lab
Exp 4 –ROM Test	**ER4 -** (- 20°) to 135° sagittal ROM	IMU reading computer	
Exp 5 – Static Stand Test	**CR1** – Support 90 kg user	Bypass Support or rail for safety Scale Lower leg prosthesis	Arc Lab
Exp 6 – Stand to Sit Test	**CR7** – Stand to sit	Chair Rail/Support Bypass Camera	Arc Lab
Exp 7 – Sit to Stand Test	**CR6** – Sit to stand	Chair Rail/Support Bypass Camera	Arc Lab
Exp 8 – Motor Torque Performance Check	**ER5** – Torque of 66.2Nm	Mounting System Weight-tension system Camera	Arc Lab
Exp 9 – Motor Cadence Performance Check	**ER6** – Cadence of 1.25 steps per second	Mounting System Weight-tension system Camera	Arc Lab

9.2 Detailed Testing Plan

9.2.1 Device Weight Check

9.2.1.1 Summary

This test will evaluate whether the total weight of the hip prosthesis meets the requirement for user comfort. The design requirement being tested is **ER2**, which specifies that the device must weigh less than 15 lbs. The test will see if the device meets that limit. A scale will be needed in order to determine the weight of the full hip prosthesis, which means there will be no necessary calculation, only direct measurement. The test will measure the weight of the manufactured piece of the device, the upper pylon, and the electronics

9.2.1.2 Procedure

1. Place the fully assembled prosthesis on the scale
2. Record measured weight
3. Repeat measurement 3 times to ensure accuracy

9.2.1.3 Results

The total device weight was found to be 10.2 lbs., well below the max threshold of 15lb. This test was successful.

9.2.2 Attachment Verification

9.2.2.1 Summary

This test verifies that the prosthesis properly interfaces with the standardized prosthetic components. The requirement tested is **CR5**, which ensures compatibility with the lamination plate and pyramid adapter. A lamination plate and female pyramid adapter are required for fit and alignment verification.

8.2.1.2 Procedure

1 Attach prosthesis to lamination plate
2 Attach pyramid adapter
3 Check alignment and secure fit

9.2.2.3 Results

Device allows for secure attachment of the female pyramid adapter. This test was successful

9.2.3 Power Usage Test

9.2.3.1 Summary

To analyze battery life reliability in use, this experiment will ensure that **ER 7** is met, providing a

minimum of 1 hour of full continuous use. To perform this experiment, a secure location and suspension of the system are needed, along with weights, and a predesigned Sit-to-Stand protocol. The goal is to measure the power used by the system using a camera pointed at a power supply with a wattage reading. The power used will then be counted frame by frame to calculate energy used by the system during its most energy intensive activity and then compare that energy to the amount stored in the systems battery to find a total usage time, fulfilling **CR 4**.

9.2.3.2 Procedure

1. Secure the device to the suspension system and suspend 11.2 pounds at .3875 m to simulate lifting Torque.
2. Record 10 Sit-to-Stand protocols, capturing the wattage each frame.
3. Calculate the allowed use of time given energy used per recorded tests.

9.2.3.3 Results

Each test took 1.433 seconds per sit to stand, and with an average recorded power of 22.41W per test, an energy of 32.12 J was recorded for each sit to stand simulation. This is above the theoretical natural energy usage of 28.8 J, but this is due to extra energy being used to power the electrical system of the device. The battery used for the system is a 36V 2.2Ah battery, giving it a total energy of 285120 J. The total amount of sit to stands that can be performed is 8876. At 1.433 seconds each, the device can perform its most energy intensive function for 3.533 hours. As that far exceeds the group's goal of 1 hour, this test was a success.

9.2.4 ROM Test

9.2.4.1 Summary

This experiment will be completed by setting the leg to mimic the IMU and the IMU angle to be read. The leg will have to move under the desired ROM on - 20° to 135° sagittal ROM without intersecting with the person that it is attached to. 0° is defined as the leg at a standing straight up position.

9.2.4.2 Procedure

1. Set motor into IMU mimic mode
2. Attempt to rotate IMU from ranges of - \20° to 135°
3. Record what the minimum and maximum angles are able to be reached by the leg without intersecting with any external bodies

9.2.4.3 Results

The leg rotates with the range of -15.11° to 120.73° before intersecting with the lamination plate it is attached to. While this range is less than that sought after in the test, upon further review with our clients, this range was determined as satisfactory, and therefore the test was successful.

9.2.5 Static Stand

9.2.5.1 Summary

Within this test we perform experiments to verify the devices' ability to support up to 90 kg or 198.4 lb. individual as seen in **CR1**. An individual wearing the prosthetic will be asked to stand on two scales for at least 30 seconds, while trying to balance an equal amount of weight on each leg. The goal is to stand for over 30 seconds while keeping the weight on each leg within 15% of the max weight

9.2.5.2 Procedure

1. Set up prosthetics to be attached to the subject by use of testing apparatus.
2. Assist individual to starting stance on the two scales
3. Begin timer as assistant removes support
4. The testing individual will stand on both the prosthetic and sound leg on top of two scales, with other group members recording the weight distribution of the leg
5. Stopping timer for 30 seconds or when an individual may fall.
6. Record data and repeat for a total of three times.

9.2.5.3 Results

Each of the three trials was a success in terms of time, as the individual stood alone for greater than 30 seconds on each test. The loadings of each leg per trial are as follows:

Table 15: Static Stand Results

Trial	Sound Leg Load (lb.)	Prosthetic Leg Load (lb.)	Load difference (%)
1	114	82.4	16.1
2	105	95.2	4.9
3	93.1	106.8	-6.8%

As can be observed the patient was able to achieve a max loading of 106.2 lbs. on the prosthetic, exceeding the goal of 50% loading, or 99.2lbs. While the percentage of our first test was greater than the maximum of 15%, this was determined to be caused by the subject not being used to the system, which can be observed by each trial having a greater loading on the prosthetic than the last. For that reason, this test was determined to be successful.

9.2.6 Stand to Sit Test

9.2.6.1 Summary

This test evaluates the controlled descent of the user during sitting, both with assistance of the sound leg, and without it. The requirement being tested is **CR7**, in which the device must allow the user to go from standing to a seated position. To conduct this test, some sort of chair or seat, safety rail/support, a bypass, an IMU, and a camera are all needed. Scales proved difficult to implement in the same way as prior tests, so the results will be determined qualitatively

9.2.6.2 Procedure

1. Equip user with prosthesis and bypass
2. Calibrate sensor to 0 degrees and set into IMU mimic mode so that the prosthetic mirrors the movement of the sound leg
3. Perform stand-to-sit action with assistance of sound leg 3 times, attempting to use it an equal amount to the prosthetic

9.2.6.3 Results

The device allows the user to sit down with relative ease. The sound leg is still carrying most of the weight while descending, but the standing to sitting transition felt smooth. For that reason, the test was determined to be successful.

9.2.7 Sit to Stand

9.2.7.1 Summary

This experiment will measure the system's ability to assist the user from a sitting position to an upright standing position; specifically, with the assistance from the sound leg. **CR 6** will be tested, in which the system must assist the user to a standing position from being seated. Scales proved difficult to implement in the same way as prior tests, so the results will be determined qualitatively

9.2.7.2 Procedure

1. Equip user with prosthesis and bypass
2. Calibrate sensor to 90 degrees and set into IMU mimic mode so that the prosthetic mirrors the movement of the sound leg
3. Perform sit-to-stand action with assistance of sound leg 3 times, attempting to use it an equal amount to the prosthetic

9.2.7.3 Results

The device was able to be used to assist the wearer in standing up from a seated position. However the wearer was only able to use the device for a small portion of the required torque needed to lift the user. This was observed to be due to how the leg was loaded onto the bypass The loading did not allow for the devices torque to be placed partially under the user like it would be with a full hip disarticulation patient, and the foot of the device being extended farther that the sound foot of the user due to the geometry of the bypass. While the groups found in later testing that the device is physically capable of lifting that weight, due to the difficulty of use during the test, the test was determined to be unsuccessful.

9.2.8 Motor Torque Performance Check

9.2.8.1 Summary

In experiment 8, we will be measuring the torque that the motor is able to lift with. The max torque in the hip happens as the leg is slowing from moving backwards and begins moving forward again. For this reason, the max torque will be tested with a velocity of 0. Our target torque is 66.2 Nm found within **ER 5**. This will be done by having the lamination plate of the device fixed to a table. Then having weight loaded to the pylon until the device cannot lift the weight or until the max torque threshold is

reached.

9.2.8.2 Procedure

1. the prosthetic to the mounting system.

2. Load a 10lb weight of 10 lbs. to the 1.2lb weight holder at a distance of 15.2 inches away from the center of rotation.

3. Use the motor to lift the leg until it is stable at 90degrees from the weight hanging off of it.

4. repeat the previous steps loading 10lbs more each time until at a final weight of 41.2lbs is loaded without failure.

9.2.8.3 Results

The leg completed each of the tests without buckling or any additional failure. Because the leg was able to hold the 41.2 lbs. stable, the max recorded torque of the device was 69.95 Nm. As this exceeds the goal of 66.2NM, this test was considered a success.

9.2.9 Cadence Test

9.2.9.1 Summary

Within this experiment, we are testing the cadence of the device as it is in use. This is for **ER6** and keeping a cadence of 1.25 steps per second. As the walking protocol was not completed, the test will be performed by loading the leg for the theoretical torque at max rotational speed for a 1.25s walk cycle. This max speed was determined to be 200 degrees per second, based off of the Bovi dataset being scaled for a faster walk speed.

9.2.9.2 Procedure

1. Toad the prosthetic to the mounting system.

2. Load a 10lb weight of 10 lbs. to the 1.2lb weight holder at a distance of 15.2 inches away from the center of rotation.

3. Set up a protocol lifting the leg from 0° to 110° at the desired speeds

4. Run the test 2 times for speed of 85 deg/s (a safe initial testing speed), 172 deg/s (the max speed of the Bovi dataset), and 200deg/s (an adjusted max speed based on our desired cadence)

9.2.9.3 Results

The leg completed each of the tests without buckling or any additional failure. Because the leg was able to lift the 11.2lbs, while at the max speed of 200 deg/s the device would be able to withstand the speeds and loadings for a walking cadence of 1.25 strides per second, and the test is determined as successful.

10 Looking Forward

Motorized prosthetics are rapidly gaining adoption in rehabilitation due to their ability to restore mobility at levels previously unattainable with passive devices. As research on this hip joint prosthetic progresses, several areas of future work present meaningful opportunities to advance both the system's performance and its contribution to the broader field.

From a mechanical standpoint, further optimization should focus on robust environmental protection and long-term durability. This includes the development of weather-resistant packaging capable of sealing sensitive components from moisture, dust, and temperature fluctuations, as well as the integration of a fully enclosed dynamic cover that accommodates joint motion without compromising protection. Material selection, fatigue analysis, and sealing strategies will be critical to ensuring reliable operation over extended use cycles, particularly in real-world conditions outside controlled laboratory environments.

On the electrical and control side, future work should prioritize the implementation of closed-loop gait intent recognition systems. Leveraging sensor fusion—such as inertial measurement units (IMUs), force sensors, and potentially electromyography (EMG)—could enable more adaptive and intuitive control strategies. In parallel, efforts to reduce signal noise and improve filtering techniques will be essential for maintaining control accuracy and responsiveness. Long-duration battery optimization also remains a key challenge; exploring higher energy-density storage, efficient power management strategies, and regenerative techniques could significantly extend operational time while minimizing system weight.

Beyond component-level improvements, system validation represents a critical next step. While initial testing with able-bodied users provides valuable baseline data, expanding trials to include individuals from the target amputee population will yield more representative performance insights. With Institutional Review Board (IRB) approval already in place, structured human subject testing can be conducted to evaluate comfort, adaptability, gait symmetry, and user confidence. These studies will not only inform iterative design improvements but also help identify unforeseen usability challenges.

Ultimately, integrating advancements in mechanical design, control systems, and user-centered validation will enhance the safety, reliability, and functionality of the prosthetic system. Continued development in these areas positions this project to contribute meaningfully to the evolution of intelligent, responsive prosthetic technologies that better meet the needs of real-world users.

11 Conclusion

The objective of this project was to design, fabricate, and validate an active powered hip prosthetic capable of improving mobility for individuals with hip disarticulation amputations. Through a structured engineering design process, the team developed a functional prototype that integrates mechanical power transmission, embedded controls, structural support, and compatibility with standard prosthetic components. Customer needs were translated into measurable engineering requirements, which guided concept generation, subsystem selection, analytical modeling, fabrication, and testing throughout the project.

Throughout this semester, with the help of our project mentors, we've established clear customer and engineering requirements to guide our design process. Mathematical analysis and iterative design improvements were used to met important requirements such as torque demand, structural loading, battery endurance, size constraints, and manufacturability. These efforts led to the successful implementation of a motor-driven hip joint that is capable of controlled motion in the sagittal plane while supporting a user's weight. Testing of the final design demonstrated that the system can improve key mobility tasks such as standing support a sit-to-stand transitions while maintaining correct operation.

Our team's collaboration with Next Step Prosthetics and participation in the NSF I-Corps Aspire Course have been an incredible asset for both the technical and financial aspects of the project. Through NSF I-Corps, we have gained insight into customer discovery and evaluation, which has been useful for gaining lots of differing insights to inform our design, as well as many networking opportunities for future potential sponsorships. Further, in working closely with Next Step Prosthetics, we have gained invaluable access to materials, knowledge and mentorship, tools and workspaces, and direct contact with a hip disarticulation patient. The combined financial and material support totaled approximately $8,000 and positioned our team exceedingly well.

One of the most significant outcomes of this project was demonstrating that a powered hip prosthetic can be developed using commercially available actuators, standard prosthetic interfaces, and custom-manufactured structural components. The final prototype represents a meaningful step beyond traditional passive hip prostheses by introducing active assistance intended to reduce compensatory movement and improve user independence. While the final build successfully met major project goals, opportunities remain for future development. Continued work should focus on gait-intent detection, closed-loop controls, reduction of system mass, improved electronics packaging, and expanded user testing with a more feasible bypass system. With these improvements, the design has strong potential to evolve into a more practical and valuable prosthesis.

Overall, this project proved the feasibility of active, single-plane, powered hip prosthesis. The team delivered a working prototype, validated core engineering principles, and established a strong technical foundation for the pursuit of creating advanced assistive prosthetic technologies.

12 References

[1] “AK80-64 KV80 Robotic Actuator - 64:1 Ratio, 120Nm Peak Torque,” CubeMars, 2025. https://www.cubemars.com/product/ak80-64-kv80-robotic-actuator.html

[2] “Ottobock,” Ottobock, 2025. *Helix3D prosthetic hip joint | Helix3D prosthesis solution* (accessed Sep. 15, 2025).

[3] “Modular Single Axis Hip Joint | Hips | Lower Limb Prosthetics | Prosthetics | Ottobock CA Shop,” *Ottobock.ca*, 2021. Available: https://shop.ottobock.ca/en/Prosthetics/Lower-Limb-Prosthetics/Hips/Modular-Single-Axis-Hip-Joint/p/7E5~5R

[4] H. J. Bennett, K. Fleenor, and J. T. Weinhandl, “A normative database of hip and knee joint biomechanics during dynamic tasks using anatomical regression prediction methods,” *Journal of Biomechanics*, vol. 81, pp. 122–131, Nov. 2018, doi:10.1016/j.jbiomech.2018.10.003.

[5] H. J. Bennett, K. Fleenor, and J. T. Weinhandl, “A normative database of hip and knee joint biomechanics during dynamic tasks using anatomical regression prediction methods,” *Journal of Biomechanics*, vol. 81, pp. 122–131, Nov. 2018, doi:10.1016/j.jbiomech.2018.10.003.

[6] E. D. Lemaire, T. J. Supan, and M. Ortiz, “Global standards for prosthetics and orthotics,” *Canadian Prosthetics & Orthotics Journal*, Oct. 2018, doi:10.33137/cpoj.v1i2.31371.

[7] G. G. Polkowski and J. C. Clohisy, “Hip biomechanics,” *Sports Medicine and Arthroscopy Review*, vol. 18, no. 2, pp. 56–62, Jun. 2010, doi:10.1097/JSA.0b013e3181dc5774.

[8] S. Au and H. Herr, “Powered ankle-foot prosthesis,” *IEEE Robotics & Automation Magazine*, vol. 15, no. 3, pp. 52–59, Sep. 2008, doi:10.1109/MRA.2008.927697.

[9] Y. Tian, A. Plummer, P. Iravani, J. Bhatti, S. Zahedi, and D. Moser, “The design, control, and testing of an integrated electrohydrostatic powered ankle prosthesis,” *IEEE/ASME Transactions on Mechatronics*, vol. 24, no. 3, pp. 1011–1022, Jun. 2019, doi:10.1109/TMECH.2019.2911685.

[10] R. Gehlhar, M. Tucker, A. J. Young, and A. D. Ames, “A review of current state-of-the-art control methods for lower-limb powered prostheses,” *Annual Reviews in Control*, Apr. 2023, doi:10.1016/j.arcontrol.2023.03.003.

[11] G. Stark, “Overview of hip disarticulation prostheses,” *Journal of Prosthetics and Orthotics*, LWW, 2025. [Online]. Available: https://journals.lww.com/jpojournal/fulltext/2001/06000/Overview_of_Hip_Disarticulation_Prostheses.14.aspx. [Accessed: Sep. 18, 2025].

[12] E. Gailledrat *et al.*, “Does the new Helix 3D hip joint improve walking of hip disarticulated amputees?,” *Annals of Physical and Rehabilitation Medicine*, vol. 56, no. 5, pp. 411–418, Jul. 2013, doi:10.1016/j.rehab.2013.05.001.

[13] F. Golshan, N. Baddour, H. Gholizadeh, and E. D. Lemaire, “A pelvic kinematic approach for calculating hip angles for active hip disarticulation prosthesis control,” *Journal of Neuroengineering and Rehabilitation*, vol. 20, no. 1, Nov. 2023, doi:10.1186/s12984-023-01273-x. [Online]. Available: https://www.ncbi.nlm.nih.gov/pmc/articles/PMC10634065/.

[14] M. Nietert, N. Englisch, P. Kreil, and G. Alba-Lopez, “Loads in hip disarticulation prostheses during normal daily use,” *Prosthetics and Orthotics International*, vol. 22, no. 3, pp. 199–215, Dec. 1998, doi:10.3109/03093649809164485.

[15] S. Mroz, N. Baddour, P. Dumond, and E. D. Lemaire, “Design and prototype validation of a laterally mounted powered hip joint prosthesis,” *Journal of Rehabilitation and Assistive Technologies Engineering*, vol. 11, Jan. 2024, doi:10.1177/20556683241248584.

[16] T. Chin, S. Sawamura, R. Shiba, H. Oyabu, Y. Nagakura, and A. Nakagawa, “Energy expenditure during walking in amputees after disarticulation of the hip: A microprocessor-controlled swing-phase control knee versus a mechanical-controlled stance-phase control knee,” *The Journal of Bone and Joint Surgery. British Volume*, vol. 87, no. 1, pp. 117–119, Jan. 2005.

[17] M. Botros, H. Gholizadeh, F. Golshan, D. Langlois, N. Baddour, and E. D. Lemaire, “Development of a powered four-bar prosthetic hip joint prototype,” *Prosthesis*, vol. 7, p. 105, 2025, doi: 10.3390/prosthesis7050105.

[18] M. S. H. Bhuiyan, I. A. Choudhury, M. Dahari, Y. Nukman, and S. Z. Dawal, “An investigation into a gear-based knee joint designed for lower limb prosthesis,” *Applied Bionics and Biomechanics*, vol. 2017, Art. no. 7595642, 2017, doi: 10.1155/2017/7595642.

[19] G. Giarmatzis, I. Jonkers, M. Wesseling, S. V. Rossom, and S. Verschueren, “Loading of hip measured by hip contact forces at different speeds of walking and running,” *Journal of Bone and Mineral Research*, vol. 30, no. 8, pp. 1431–1440, 2015, doi: 10.1002/jbmr.2483

[20] P. R. Golyski, B. K. Potter, J. A. Forsberg, and B. D. Hendershot, “Comparing the Mechanical Energetics of Walking Among Individuals with Unilateral Transfemoral Limb Loss Using Socket and Osseointegrated Prosthetic Interfaces,” *Scientific Reports*, vol. 15, no. 1, Art. no. 9755, 2025, doi: 10.1038/s41598-025-93211-1.

[21] T. Kawaguchi, T. Yamada, and K. Iwashita, “Biomechanical gait analysis for a hip disarticulation prosthesis: power source for the swing phase of a hip disarticulation prosthetic limb,” *Journal of Physical Therapy Science*, vol. 35, no. 5, pp. 361–365, 2023, doi:10.1589/jpts.35.361.

[22] X. Li, Z. Deng, Q. Meng, S. Bai, W. Chen, and H. Yu, “Design and optimization of a hip disarticulation prosthesis using the remote center of motion mechanism,” *Technology and Health Care*, pp. 1–13, Jun. 2020, doi:10.3233/THC-192088.

[23] P. P. Bonato, *Wearable Robotics: Challenges and Opportunities*, Springer, 2018.

[24] American Gear Manufacturers Association (AGMA), “Standards & Emerging Technology,” *AGMA.org*, 2025. [Online]. Available: https://www.agma.org/standards-technology/. [Accessed: Sep. 18, 2025].

[25] K. B. Fite, “Overview of the components used in active and passive lower-limb prosthetic devices,” in *Full Stride*, V. Tepe and C. Peterson, Eds., Springer, 2017, doi:10.1007/978-1-4939-7247-0_4.

[26] S. M. Zaffer, R. L. Braddom, A. Conti, J. C. Goff, and D. C. Bokma, “Total hip disarticulation prosthesis with suction socket: Report of two cases,” *American Journal of Physical Medicine & Rehabilitation*, vol. 78, no. 2, pp. 160–162, Mar. 1999.

[27] F. A. Gottschalk and M. Stills, “The biomechanics of trans-femoral amputation,” *Prosthetics and Orthotics International*, vol. 18, no. 1, pp. 12–17, Apr. 1994, doi:10.3109/03093649409164665.

[28] G. Bovi, M. Rabuffetti, P. Mazzoleni, and M. Ferrarin, “A multiple-task gait analysis approach: Kinematic, kinetic and EMG reference data for healthy young and adult subjects,” *Gait & Posture*, vol. 33, no. 1, pp. 6–13, 2011, doi:10.1016/j.gaitpost.2010.08.009.

[29] A. J. Young and D. P. Ferris, “State of the art and future directions for lower limb robotic exoskeletons,” *IEEE Transactions on Neural Systems and Rehabilitation Engineering*, vol. 25, no. 2, pp. 171–182, Feb. 2017, doi:10.1109/TNSRE.2016.2521160.

[30] D. E. Geiger, F. Behrendt, and C. Schuster-Amft, “EMG muscle activation pattern of four lower extremity muscles during stair climbing, motor imagery, and robot-assisted stepping: a cross-sectional study in healthy individuals,” *BioMed Research International*, vol. 2019, pp. 1–8, Mar. 2019, doi:10.1155/2019/9351689.

[31] L. Guo *et al.*, “On the design evolution of hip implants: A review,” *Materials & Design*, vol. 216, no. 110552, Apr. 2022, doi:10.1016/j.matdes.2022.110552.

[32] D. Dalli, J. Buhagiar, P. Mollicone, and P. Schembri Wismayer, “A novel hip joint prosthesis with uni-directional articulations for reduced wear,” *Journal of the Mechanical Behavior of Biomedical Materials*, vol. 127, p. 105072, Mar. 2022, doi:10.1016/j.jmbbm.2021.105072.

[33] J. Nilsson and A. Thorstensson, “Ground reaction forces at different speeds of human walking and running,” *Acta Physiologica Scandinavica*, vol. 136, no. 2, pp. 217–227, Jun. 1989,

doi:10.1111/j.1748-1716.1989.tb08655.x.

[34] “Shijiazhuang Perfect Prosthetic Manufacture Co., Ltd.,” *Shijiazhuang Perfect Prosthetic Manufacture Co., Ltd.*, 2025. [Online]. Available: https://www.sjzpfc.com/product-square-adapter-with-pyramid.html.

[35] A. Kharb, V. Saini, Y. K. Jain, and S. Dhiman, “A review of gait cycle and its parameters,” *ResearchGate*, Jan. 2011. [Online]. Available: https://www.researchgate.net/publication/268423123_A_review_of_gait_cycle_and_its_parameters.

[36] Boston Gear, *Boston Gear Product Catalog P-1930-BG*. Quincy, MA: Boston Gear, 2019. Accessed: Nov. 22, 2025.

[37] Boston Gear, “H610R Steel Helical Gear,” *Power Motion & Industrial Supplies*, Yakima, WA, USA. Available: https://pmisupplies.com/products/h610r-boston?srsltid=AfmBOopTI6H_BglRNie6a6LBGJJbulZuWcMDOuiC0LYGearGSgnZurqY. [Accessed: Nov. 22, 2025].

[38] Not a possible IEEE citation, but a link to the listed battery https://www.amazon.com/DFTIM-36V-Replacement-Hoverboard Configuration/dp/B0F5QF3Y23/ref=sr_1_5?crid=IQO7KYW02MEB&dib=eyJ2IjoiMSJ9.mxMr7FHO7IMqOHCSJy5VPTxZ0WjO3viewHjy3QOkU3qrnKXXt4MPlgI8cfwvCxQ4fT0FQ0C0EzZfD4BeuRpOGpN26xSLthMM9HEPJ9fdQCnErK4Hic0wXtnKeb29wYheQ7e34i5coKst97G6_yIQkfYZXsgrtIdVHhh93kQUhO91gzsV1qt-F93GMlWivNXuLQwSnry4N6luHVD2T6j13oGPIuJbTg_SE5HdfEdlVKA51ugEebFyPruLTlfc1JS5Tjorj10SPv2V7SMnd1ejcCQGrpzgrh0YaO8XQxE.rn3BmjKa95FjgpdARbP2H4pOy7C4KeKi6aDDHs5QxI8&dib_tag=se&keywords=36v+4400mah+battery&qid=1763873497&sprefix=36V+44%2Caps%2C118&sr=8-5

13 APPENDICES

a. Appendix A: Motor Analysis MATLAB Program

```
BW = 90;
torque = -BW*bovi.adult.normal.hip.sagittal.torque(:,2);
rms(torque) % for hip joint for continuous / gear ratio
position = bovi.adult.normal.hip.sagittal.position(:,2);
stride_time = 1.2;
time = linspace(0, stride_time, length(torque));
close all
subplot(311); plot(time,torque); % Flexion
subplot(312); plot(time,position); % Extension
subplot(313); plot(position, torque);
pos_rad = deg2rad(position);
vel_rad = dfdx(time,pos_rad);
acc_rad = dfdx(time,vel_rad);
close all
subplot(211); plot(time, vel_rad)
subplot(212);plot(time, vel_rad.*torque)
GR = 15;
motor_inertia = 579/10^7;
kt = .09;
R = .160;
vel_motor = vel_rad*GR;
tor_motor_static = torque/GR;
tor_motor_dynamic = motor_inertia*acc_rad*GR;
current = (tor_motor_static + tor_motor_dynamic)/kt;
volts = current*R + kt*vel_motor;
close all;
subplot(3,1,1); plot(time, volts);
subplot(3,1,2); plot(time, current);
subplot(3,1,3); plot(time, volts.*current)
close all;
% speed torque curve
plot(abs(current*kt), abs(vel_motor)); ylabel("motor speed rad/s");
   xlabel("Motor Torque Nm"); hold on;
w_limit = [570, 0]*2*pi/60;
t_limt = [0, 22];
plot(t_limt, w_limit, 'k'); hold off
GR = 25:45;
motor_inertia = 579/10^7;
kt = .09;
```

```
52 R = .160;
53 vel_motor = vel_rad.*GR;
54 tor_motor_static = torque./GR;
55 tor_motor_dynamic = motor_inertia.*acc_rad.*GR;
56
57 current = (tor_motor_static + tor_motor_dynamic)./kt;
58 volts = current.*R + kt.*vel_motor;
59 e_power = current.*volts;
60
61 i_max = max(abs(current));
62 i_rms = rms(current);
63 v_max = max(abs(volts));
64 p_max = max(abs(e_power));
65
66 close all;
67 subplot(411); plot(GR, i_max); ylabel("Amps"); hold on; yline(28); % peak
   current limit
68 subplot(412); plot(GR, i_rms); ylabel("Amps"); hold on; yline(12); %
   continuous current limit
69 subplot(413); plot(GR, v_max); ylabel("Volts"); hold on; yline(48); % votlage
   limit
70 subplot(414); plot(GR, p_max); ylabel("Power");
```

b. Appendix B: Figures

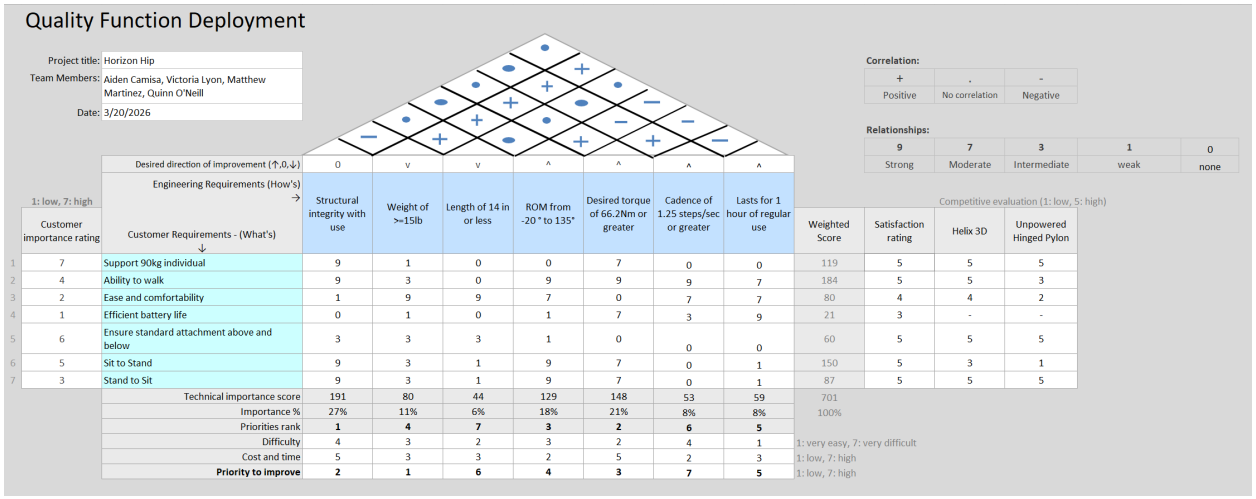

Quality Function Deployment

Project title: Horizon Hip
Team Members: Aiden Camisa, Victoria Lyon, Matthew Martinez, Quinn O'Neill
Date: 3/20/2026

Correlation:

+	.	-
Positive	No correlation	Negative

Relationships:

9	7	3	1	0
Strong	Moderate	Intermediate	weak	none

	Customer importance rating (1: low, 7: high)	Customer Requirements - (What's)	Engineering Requirements (How's) →	Structural integrity with use	Weight of >=15lb	Length of 14 in or less	ROM from -20 ° to 135°	Desired torque of 66.2Nm or greater	Cadence of 1.25 steps/sec or greater	Lasts for 1 hour of regular use	Weighted Score	Satisfaction rating	Competitive evaluation (1: low, 5: high) Helix 3D	Unpowered Hinged Pylon
		Desired direction of improvement (↑,0,↓)		0	v	v	^	^	^	^				
1	7	Support 90kg individual		9	1	0	0	7	0	0	119	5	5	5
2	4	Ability to walk		9	3	0	9	9	9	7	184	5	5	3
3	2	Ease and comfortability		1	9	9	7	0	7	7	80	4	4	2
4	1	Efficient battery life		0	1	0	1	7	3	9	21	3	-	-
5	6	Ensure standard attachment above and below		3	3	3	1	0	0	0	60	5	5	5
6	5	Sit to Stand		9	3	1	9	7	0	1	150	5	3	1
7	3	Stand to Sit		9	3	1	9	7	0	1	87	5	5	5
		Technical importance score		191	80	44	129	148	53	59	701			
		Importance %		27%	11%	6%	18%	21%	8%	8%	100%			
		Priorities rank		**1**	**4**	**7**	**3**	**2**	**6**	**5**				
		Difficulty		4	3	2	3	2	4	1	1: very easy, 7: very difficult			
		Cost and time		5	3	3	2	5	2	3	1: low, 7: high			
		Priority to improve		**2**	**1**	**6**	**4**	**3**	**7**	**5**	1: low, 7: high			

Figure 2: Quality Function Deployment

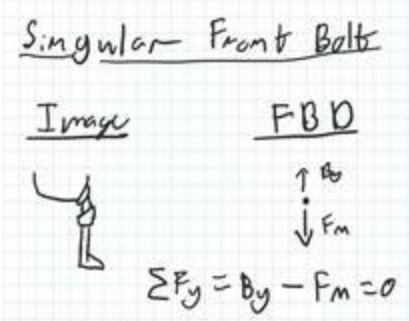

Figure 2: Free-body Diagram of Prosthetic

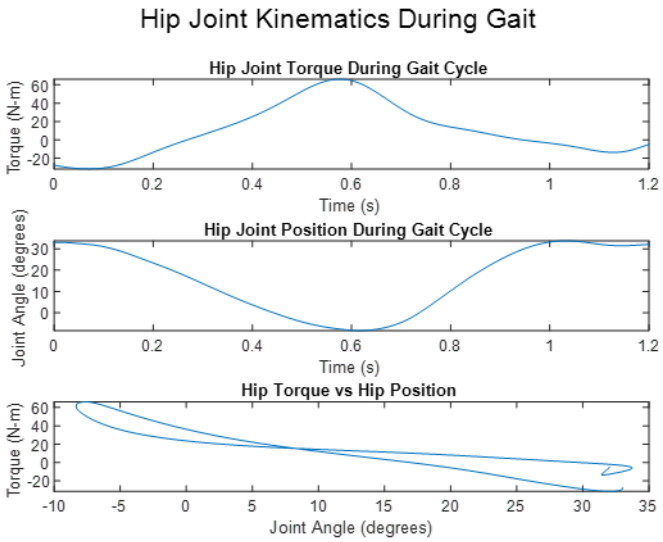

Figure 3: Hip Joint Kinematics During Gait Cycle

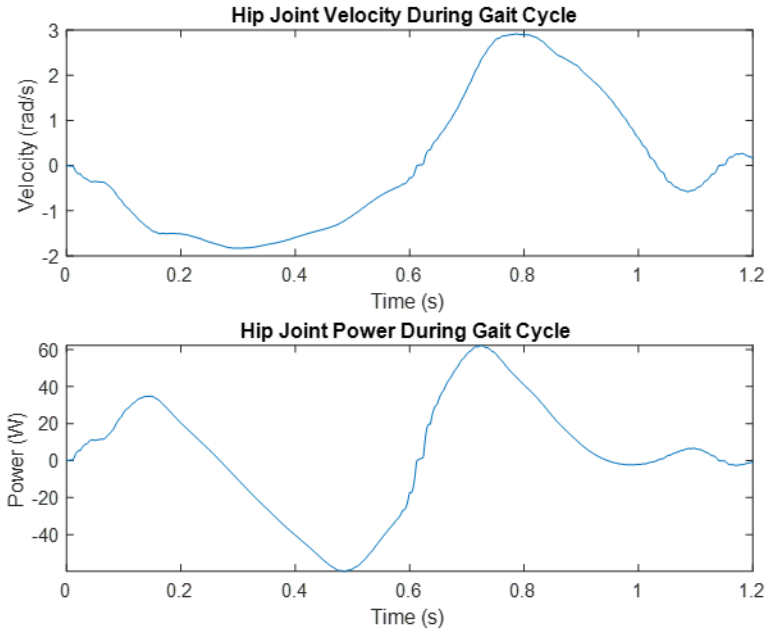

Figure 4: Hip Joint Velocity and Power During Gait Cycle

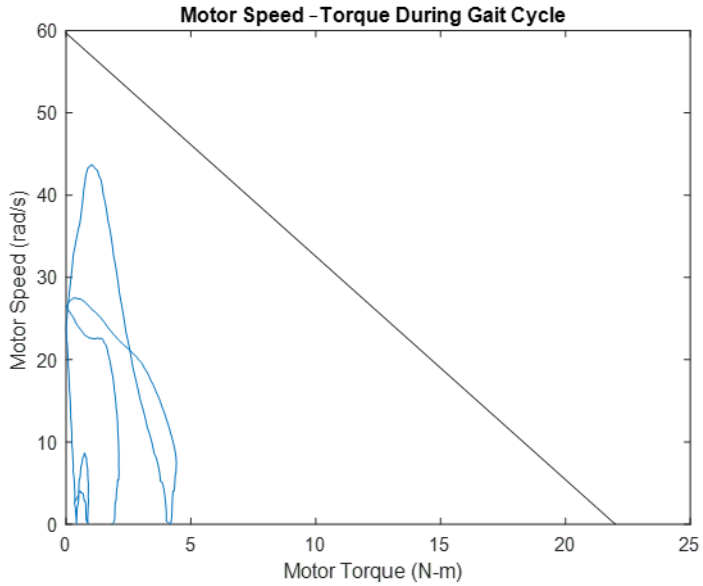

Figure 5: Motor Speed-Torque During Gait

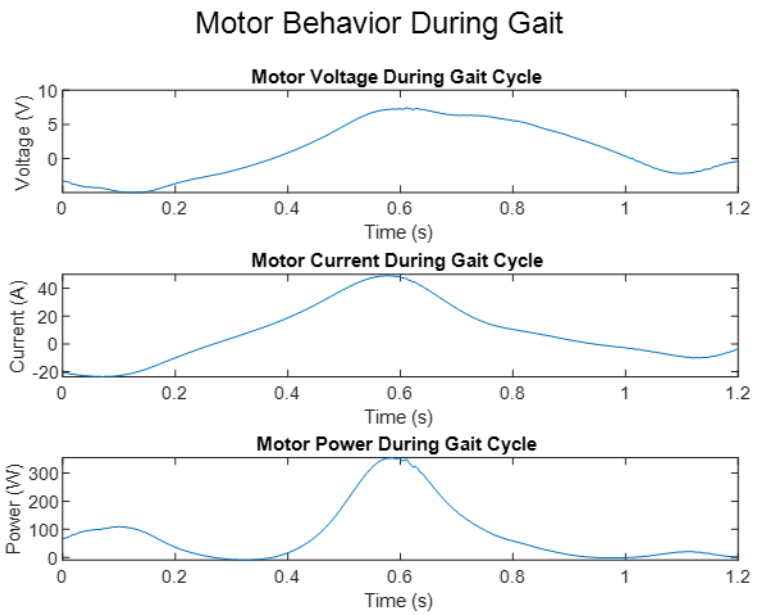

Figure 6: Motor Behavior During Gait

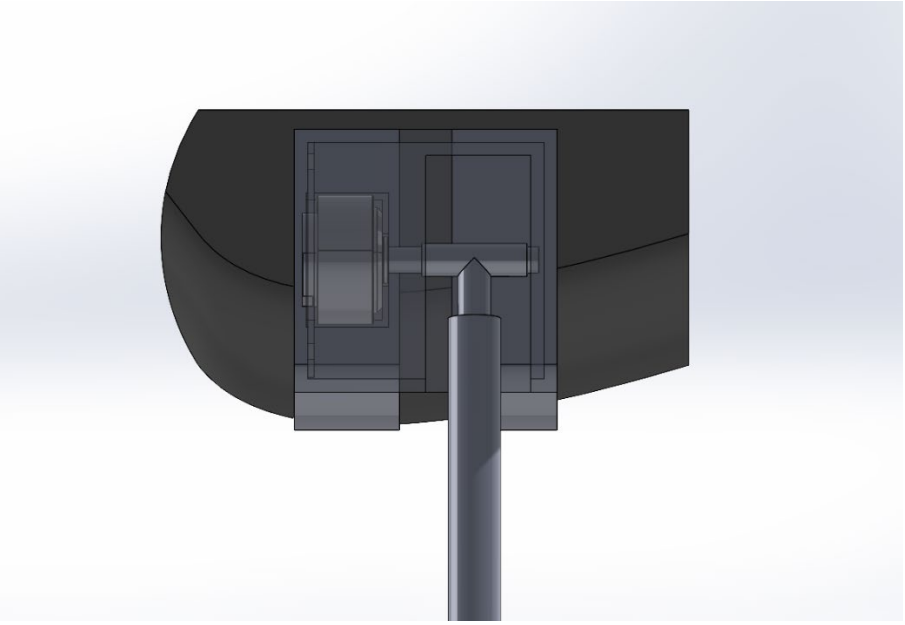

Figure 7: Initial Prototype Design

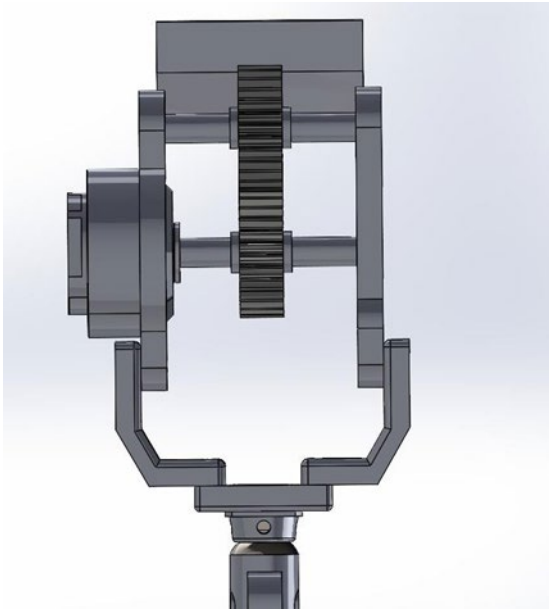

Figure 8: Current Prosthesis Design

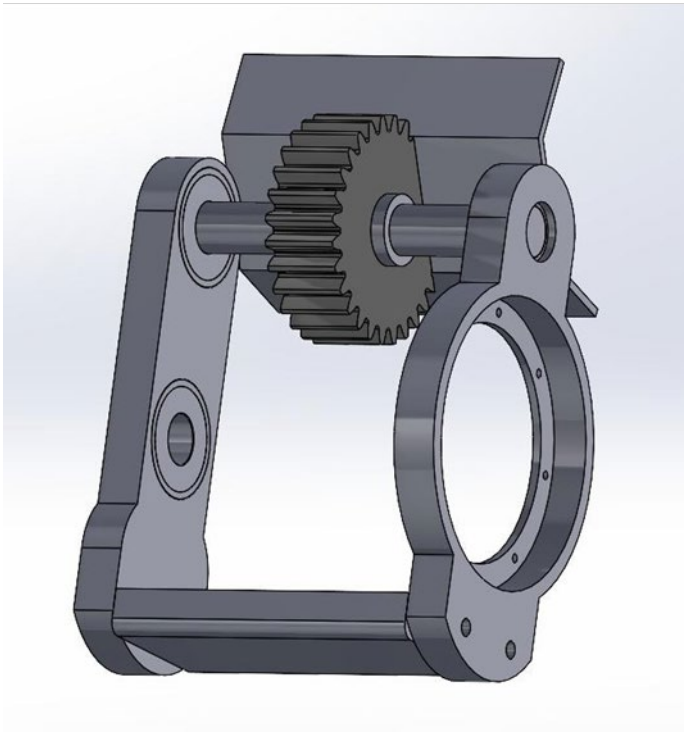

Figure 9: New Frame Design Model

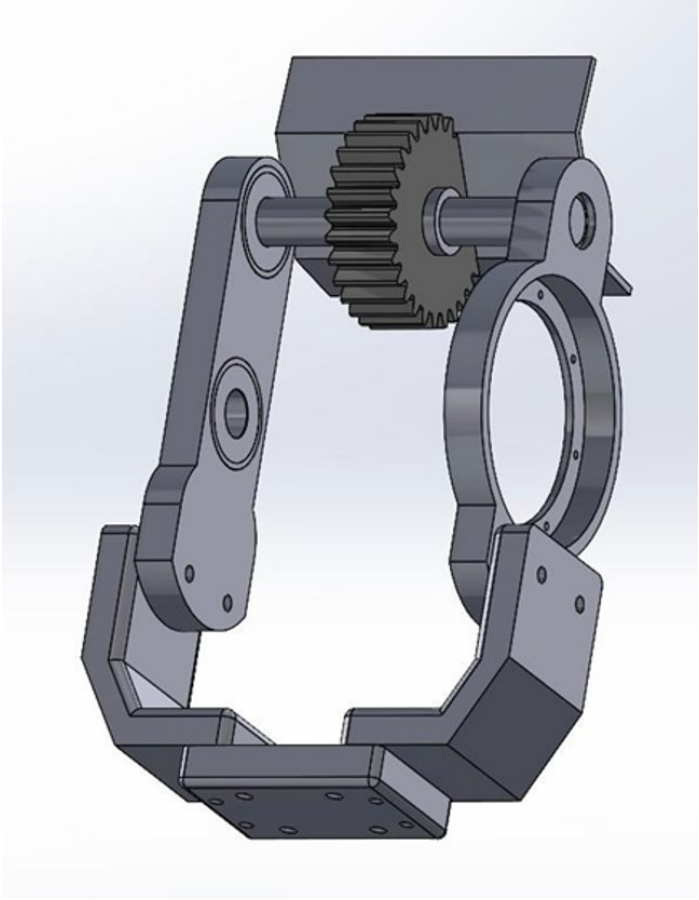

Figure 10: Current Frame Design Model

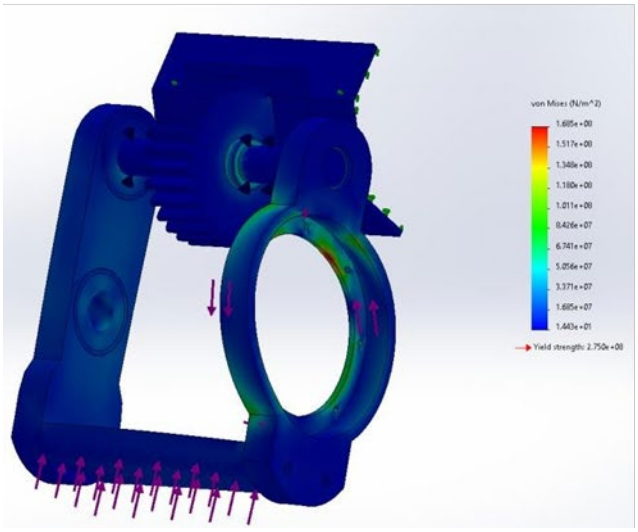

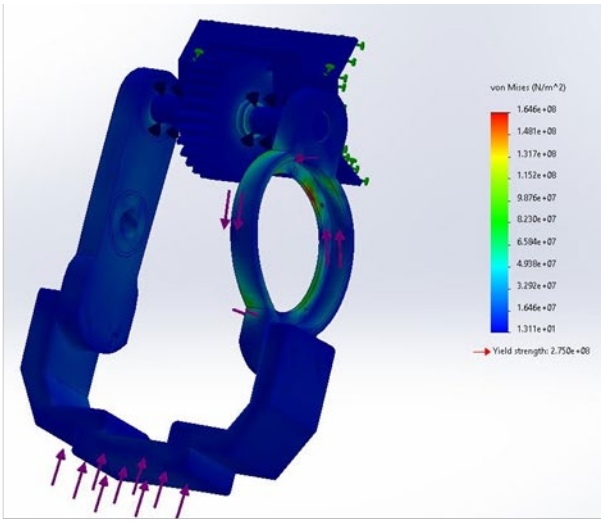

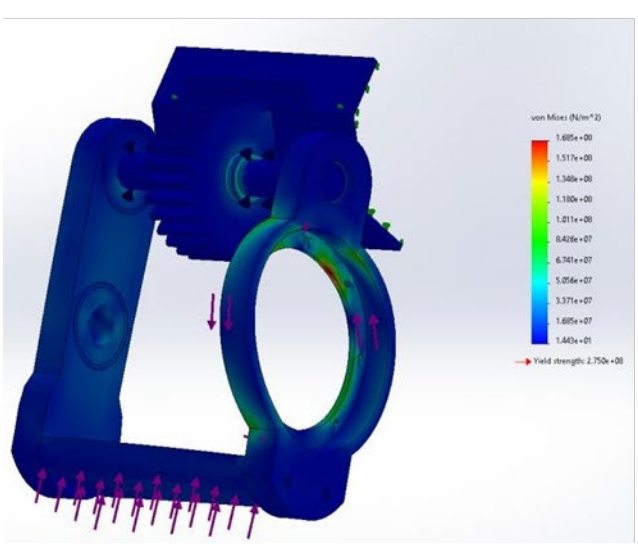

Figure 11: Stress for New design

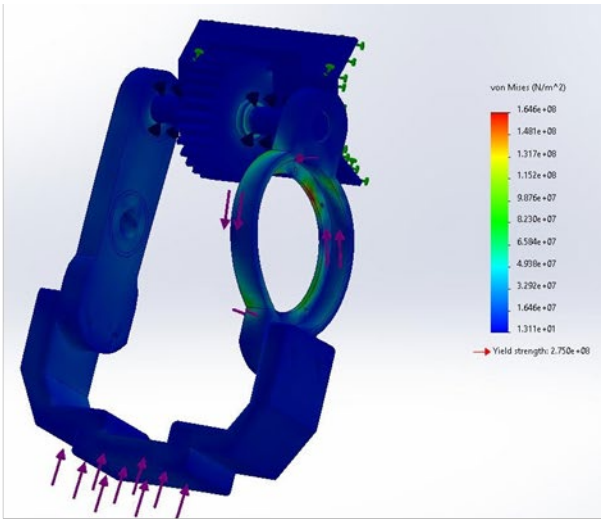

Figure 12: Stress for Current design

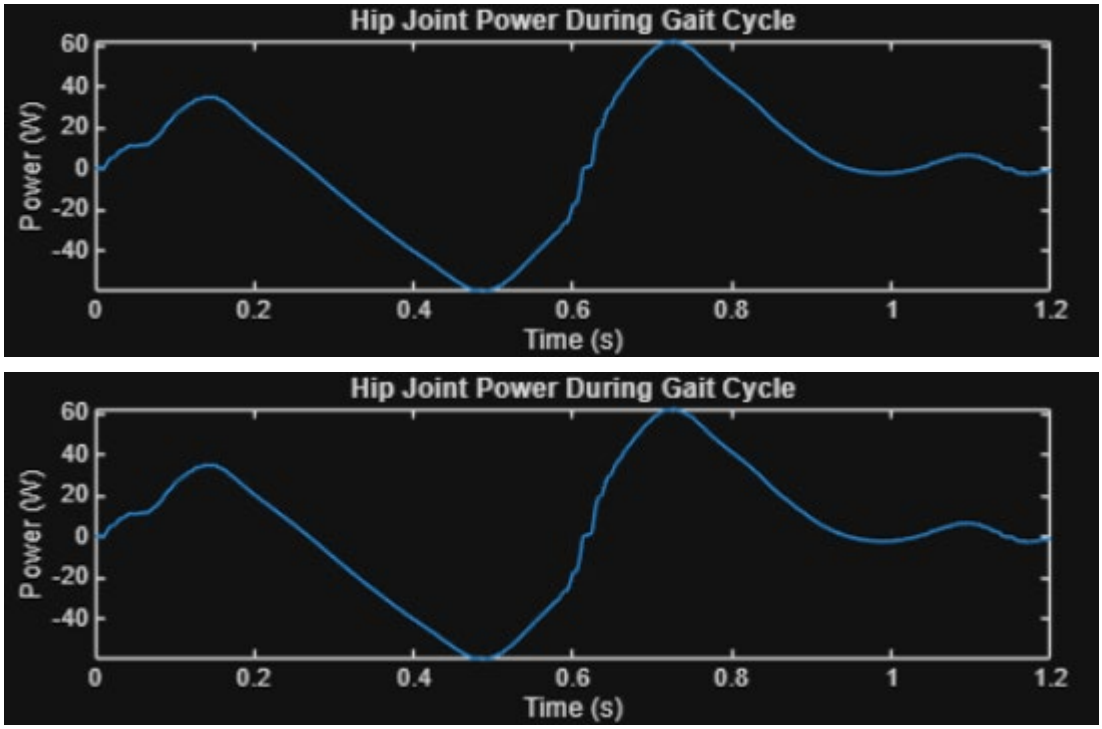

Figure 13: Hip joint power per gait time

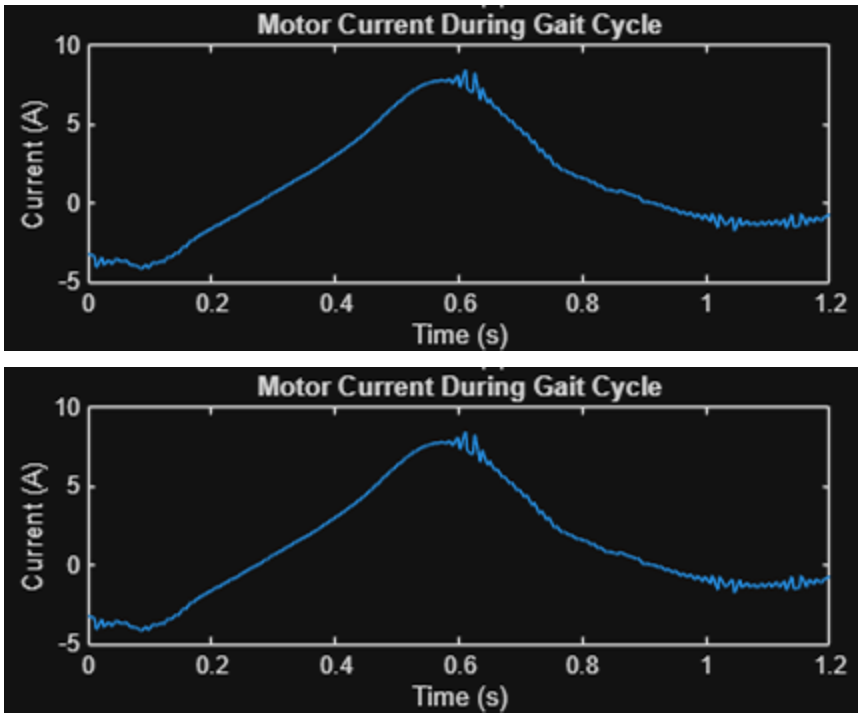

Figure 14: Motor current per gait time

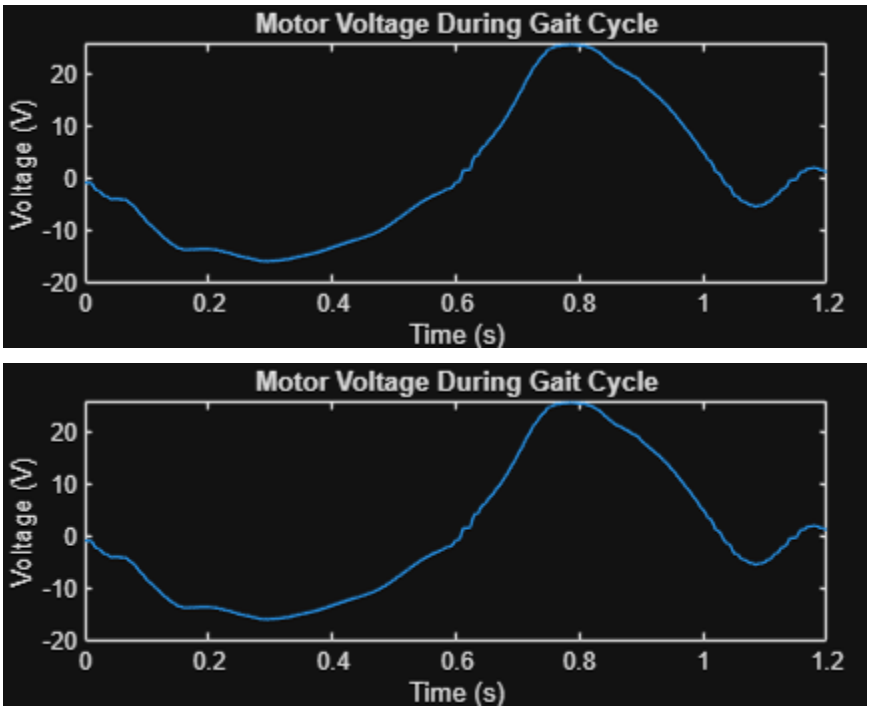

Figure 15: Motor Voltage per gait time

Figure 16: Selected battery for the team

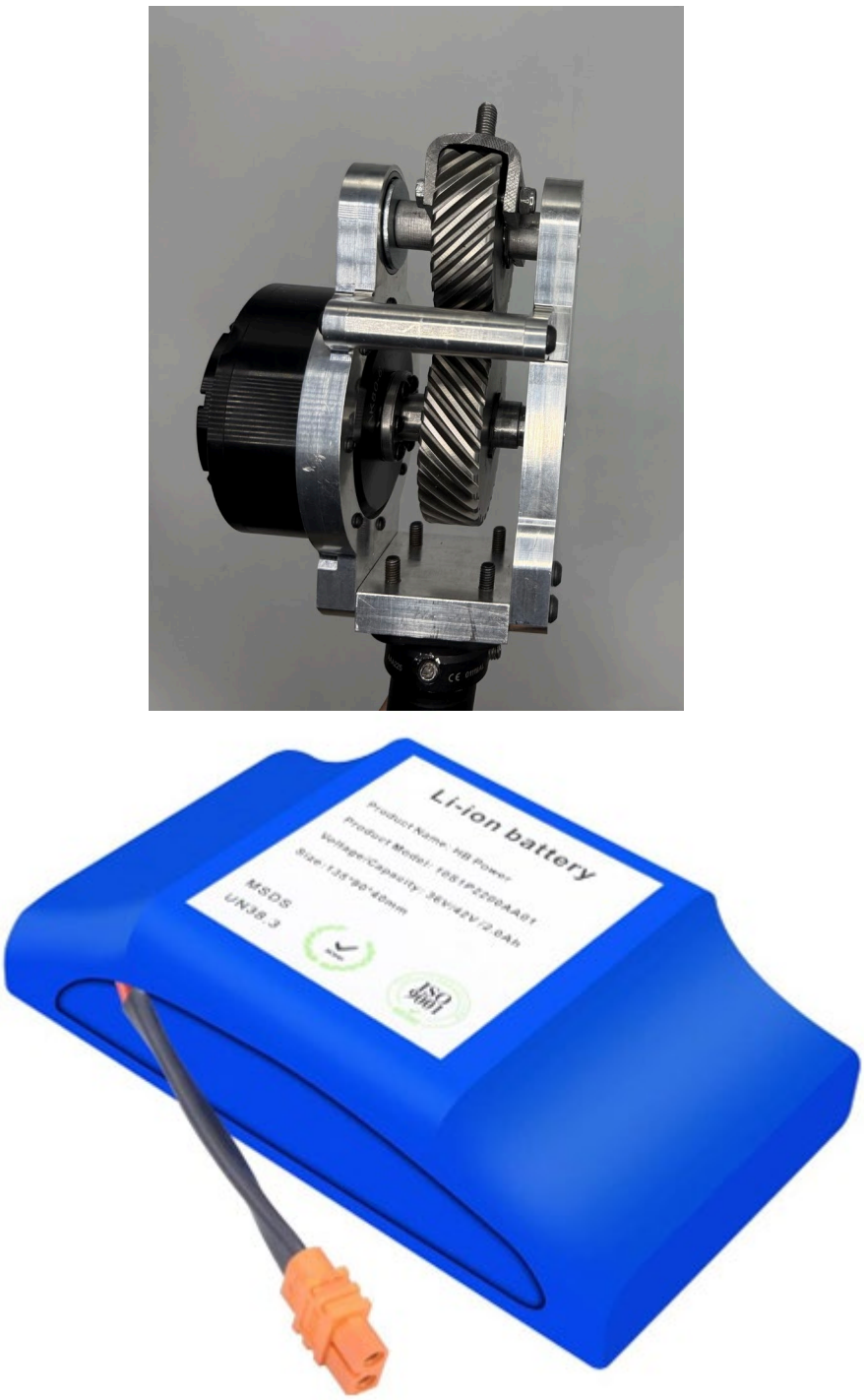

Figure 16: Selected battery for the team

Figure 17: Final Assembly

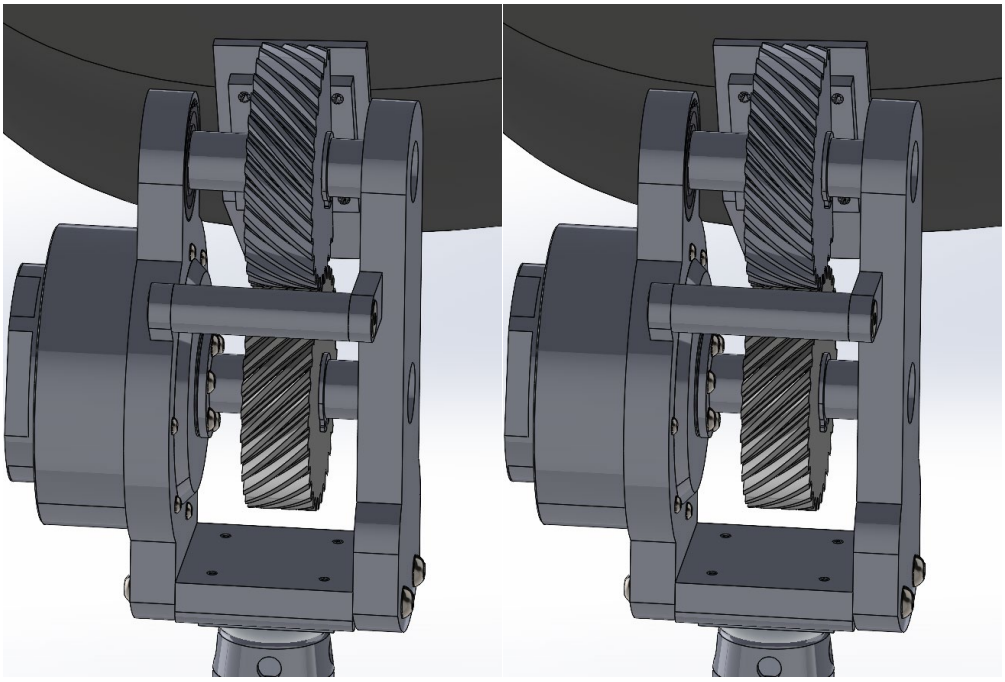

Figure 18: Final CAD Model

Figure 19: Bench Test Setup

Figure 20: Hip Immobilizing Bypass

Figure 21: Complete Functional Testing Setup

Figure 22: System Cover

c. *Appendix C: Tables*

Table 1: Summary of Engineering Requirements

Requirement	Target
ER 1: Durable	≥ 18 load test cycles
ER 2: Lightweight	< 15 lbs
ER 3: Compact	≤ 14 in length
ER 4: Range of Motion	-20° to 135°
ER 5: Torque	66.2 Nm
ER 6: Cadence	1.25 steps/sec
ER 7: Energy	Within 20% of natural energy used

Table 2: Battery Sizing for Active Hip Prosthetic

Time (Min)	Battery required (Wh)
10	21.73
20	43.46
30	65.19
45	97.79
60	130.38
90	195.57

Table 3: Comparison of Attachment Designs

Type	Force (N)	Moment (N*m)	Force per Bolt (N)	Bearing Stress (MPa)	Shear Stress in the bolt (MPa)
Dual Attachment	882.90	52.974	441.45	13.80	8.78
Laterally Mounted	882.90	70.632	882.90	27.59	17.56
Singular Front Bolt	882.90	88.29	882.90	27.59	17.56
Angled Corner	882.90	105.948	882.90	27.59	17.56

Table 4: von Mises Stress Calculations for Potential Shaft Materials

Results	Aluminum (6061)	Titanium (Grade 4)
σ'_a	336.25 MPa	340.71 MPa
σ'_m	.0382 MPa	.0425 MPa
σ'_{max}	336.29 MPa	340.75 MPa

Table 5: Semester 1 Functional Decomposition Table

Component	1	2	3	4
Actuation	Electronic Linear actuator	Series Elastic Actuators	Rotary Actuator	Variable Stiffness Actuator
Power Transmission	Gear system	Cable	Electrostatic clutch	Belt
Mechanisms	Stewart platform with 2 Links	Ball Joint	Universal Joint	Rigid Links
Suspension / Attachment Configuration	Dual attachment [2 components bolted to the socket]	Lateral [side socket attachment]	Singular front bolt [typical use]	Angled alignment [lower corner attachment,

Table 6: Completed Bill of Materials

Hip Prosthetic Bill of Materials

Category	Item No.	Description	Primary Vendor	Unit Price	Quantity	Make/Buy	Manufacturer	Lead Time	Part Status
Main Assembly	1	AK80-64 KV80 Motor	CubeMars	$ 911.77	1	Buy	CubeMars		In-Hand
Main Assembly	2	Angular Contact Bearing	BearingsDirect	$ 13.54	3	Buy	NTN Bearings	3-4 Weeks	In-Hand
Main Assembly	3	1030L Gear	Zoro	$ 200.00	1	Buy	Boston Gears	2-3 Weeks	In-Hand
Main Assembly	4	1030R Gear	Zoro	$ 195.00	1	Buy	Boston Gears	2-3 Weeks	In-Hand
Main Assembly	5	Upper Shaft	NAU Machine Shop	$ 7.21	1	Make	Quinn	2 days	In-Hand
Main Assembly	6	Lower Shaft	NAU Machine Shop	$ 7.21	1	Make	Victoria	4 days	In-Hand
Main Assembly	7	Retaining Ring	DSR	$ -	2	Buy	Hillman	1 Week	In-Hand
Main Assembly	8	Shaft Key	Amazon	$ 3.25	2	Buy	dmiotech	3-4 Weeks	In-Hand
Main Assembly	9	Frame (Motor Side)	McMaster-Carr	$ 146.01	1	Buy	Red Rock Manufacturing	3-4 Weeks	In-Hand
Main Assembly	10	Frame (Bearing Side)	McMaster-Carr	$ 131.55	1	Buy	Red Rock Manufacturing	3-4 Weeks	In-Hand
Main Assembly	11	Lamination Plate	NextStep Prosthetics	$ -	1	Buy	Ottobock	5 days	In-Hand
Main Assembly	12	Base Plate	McMaster-Carr	$ 16.02	1	Make	Aiden	3-4 Weeks	In-Hand
Main Assembly	13	Male Pyramid Adapter	Ebay	$ 25.00	1	Buy	Trulife	N/A	In-Hand
Main Assembly	14	Structure Enforcing Bar	NAU Machine Shop	$ 10.17	1	Make	Victoria	3-4 Weeks	In-Hand
Hardware	15	M6-1x25 Socketcap Head Screw	Amazon	$ 19.99	4	Buy	Everbilt	1 Week	In-Hand
Hardware	16	M6-1x15 Socketcap Head Screw	Amazon	$ -	2	Buy	Fgruh	10 days	In-Hand
Hardware	17	M3x12 Socket Cap Head Screw	Amazon	$ -	8	Buy	Fgruh	10 days	In-Hand
Hardware	18	M4x10 Socket Cap Head Screw	Amazon	$ -	6	Buy	Fgruh	10 days	In-Hand
Hardware	19	M8x20mm Countersunk Screw	HomeDepot	$ 2.67	2	Buy	Everbilt		In-Hand

Hardware	20	M6x35 Countersunk Screw	Ebay	$ -	4	Buy	Trulife	10 days	In-Hand
Electronics	21	Adafruit CAN Controller	Adafruit	$ 19.95	1	Buy	Adafruit	2-3 Weeks	In-Hand
Electronics	22	MicroSD Card	Adafruit	$ 13.69	2	Buy	Adafruit	2-3 Weeks	In-Hand
Electronics	23	Buck Converter	Amazon	$ 15.99	1	Buy	YABOANG	1 Week	In-Hand
Electronics	24	Breadboard Jumper Wire	Amazon	$ 10.99	1	Buy	TODOELEC	5 days	In-Hand
Electronics	25	IMU Sensor	Adafruit	$ 6.99	2	Buy	HiLetgo	5 days	In-Hand
Electronics	26	RUBIK Link V2.0	CubeMars	$ 40.00	1	Make	CubeMars		In-Hand
Electronics	27	CAN Bus HAT	Waveshare	$ 39.99	1	Buy	Waveshare		In-Hand
Electronics	28	36V Battery	Amazon	$ 32.83	1	Buy	Amazon		In-Hand
Electronics	29	Battery Adapter	Amazon	$ 5.82	1	Buy	Amazon		In-Hand

Table 7: Completed Manufacturing Plan

Hip Prosthetic Bill of Materials [MANUFACTURING]

Category	Item No.	Description	Primary Vendor	Location	Quantity	Machinist	Process	Time Spent (Hrs)	Estimated Time	Progress %	Part Status
Main Assembly	9	Frame (Motor Side)	McMaster-Carr	NAU Machine Shop	1	Ryan, Red Rock	CNC	1	1	100%	In-Hand
Main Assembly	10	Frame (Bearing Side)	McMaster-Carr	NAU Machine Shop	1	Ryan, Red Rock	CNC	1	1	100%	In-Hand
Main Assembly	12	Base Plate	McMaster-Carr	NAU Machine Shop	1	Matt/Aiden	Mill	5	3	100%	In-Hand
Main Assembly	14	Structure Enforcing Bar	McMaster-Carr	NAU Machine Shop	1	Victoria	Lathe	4	2	100%	In-Hand
Main Assembly	5	Upper Shaft	NAU Machine Shop	NAU Machine Shop	1	Quinn / Aiden	Lathe, Mill	5	3	100%	In-Hand
Main Assembly	6	Lower Shaft	NAU Machine Shop	NAU Machine Shop	1	Victoria / Aiden	Lathe, Mill	7	4	100%	In-Hand
Main Assembly	11	Mounting Bracket	McMaster-Carr	NAU Machine Shop	1	Matt	Mill	5	1	100%	In-Hand

Main Assembly	3	1030L Gear	Zoro	East Valley Precision Machining	1	East Valley	Wire EDM Cutting	1	1	100%	In-Hand
	3	1030L Gear	Zoro	NAU Machine Shop	0	Matt	Mill	1	1	100%	In-Hand

1. Identify					2. Classify				3. Take action				4. Action results				
Item (component, part, assembly)	Function	Requirements	Failure mode	Effect(s) of potential failure	**Severity**	**Classification**	Potential causes of failure	Current design controls (prevention)	**Occurrence likelihood**	Current design controls (detection)	**Effectiveness of best method of detection control**	**RPN (Risk priority no.)**	Recommended action(s)	**Severity**	**Occurrence**	**Detection**	**RPN (Risk priority no.)**
Motor	Providing torque to the shaft	Motor must provide enough torque, smooth, accurate torque/positioning	Control instability or sustained vibration during gait	User discomfort, reduced balance, risk of fall, joint wear	9	Safety	Poor control tuning, insufficient damping	Torque limits, firmware control	3	Manual Testing, Encoder	3	81	Implement rate limits, use high-rate inner current/torque loop	9	2	2	36
Motor	Providing torque to the shaft	Motor must provide enough torque	Motor cannot meet required torque to lift leg	Leg stops moving	4	Product failure	Motor is defunct	Product testing, inspection	1	Torque monitor, current sensing	1	4	Maintenance schedule	5	4	3	60
Motor Shaft	Power Transmission	Transmit movement	Detaches from motor	Hinders rotation	10	Safety	Fastener failure, vibration	Motor casing, using standard bolts	3	Gait stability	4	120	Include repair kit, include fasteners or clamps with design.	10	2	2	40
Motor Shaft	Power Transmission	Handles load	Shaft breaks	Joint & leg detaches	10	Safety	Material failure	Material Selection, mathematical modeling	2	Gait stability	4	80	Replace shaft, bring to prosthetist	5	3	3	45
Battery	Provide Power to the motor	Provides enough power for the motor to allow it to produce the required torque	Does not reach required power	The motor doesn't power the leg, and the leg is not able to reach the required gate	4	Product failure	Dysfunctional battery. Low power battery.	Mathematically determines the amount of power required for the motor	1	Low voltage alarm in testing	1	4	Use battery with 20-30% capacity margin	5	4	3	60
Battery	Provide Power to the motor	Provides enough power for the motor to allow it to produce the required torque	Wires break / detach from motor	Leg stops moving with power. potential danger with loose wires	6	Safety	wires not secured tightly	Clips built into motor, and no major movement of motor or battery, and sealing of the wires to the mold	3	Motor stops working, look at wire	2	36	secure wires closely to the mold to prevent damage and movement	7	3	2	36

Raspberry Pi Controller (Electrical system)	Acts as a computer to provide control	Simple and easy Interface	No Control of leg	Locks in place or becomes frozen in place. Possible tripping and injury	4	Product failure	Code is wrong or something is unplugged	Raspberry pie with a CAN bus attachment to the motor.	4	Testing the code and wiring before using it on a individual	5	80	Implement a test sequence to make sure everything works.	4	4	1	16
Attachment Plate	Suspend system on socket	Securely hold system without movement	Detaches from socket	System detaches	10	Safety	Extreme wear, unforeseen force	Secure standard fasteners	2	Stability, inspection	3	60	Safety test, user manual	5	4	3	60

Table 9: Y Factor for Spur Gears

Number of Teeth	14-1/2° Full Depth Involute	20° Full Depth Involute
10	0.176	0.201
11	0.192	0.226
12	0.210	0.245
13	0.223	0.264
14	0.236	0.276
15	0.245	0.289
16	0.255	0.295
17	0.264	0.302
18	0.270	0.308
19	0.277	0.314
20	0.283	0.320
22	0.292	0.330
24	0.302	0.337
26	0.308	0.344
28	0.314	0.352
30	0.318	0.358
32	0.322	0.364
34	0.325	0.370
36	0.329	0.377
38	0.332	0.383
40	0.336	0.389
45	0.340	0.399
50	0.346	0.408
55	0.352	0.415
60	0.355	0.421
65	0.358	0.425
70	0.360	0.429
75	0.361	0.433
80	0.363	0.436
90	0.366	0.442
100	0.368	0.446
150	0.375	0.458
200	0.378	0.463
300	0.382	0.471
Rack	0.390	0.484

Table 10: Y Factor for Helical Gears

FOR 14-1/2°PA—45° HELIX ANGLE GEAR			
No. of Teeth	Factor Y	No. of Teeth	Factor Y
8	.295	25	.361
9	.305	30	.364
10	.314	32	.365
12	.327	36	.367
15	.339	40	.370
16	.342	48	.372
18	.345	50	.373
20	.352	60	.374
24	.358	72	.377

Table 11: Spur Gear Specifications with Pressure Angle of 14.5

Teeth	Power (HP)	Torque (lb-in)	P (Teeth/in)	Face Width (in)	Diameter (in)	Volume (in^3)	Torque per Unit Volume (T/V)
25	.29	742	10	1	2.5	4.91	151.12
11	.38	946	6	1.5	1.83	3.95	239.49
16	.31	778	8	1.25	2	3.93	197.96

Table 12: Spur Gear Specifications with Pressure Angle of 20

Teeth	Power (HP)	Torque (lb-in)	P (Teeth/in)	Face Width (in)	Diameter (in)	Volume (in^3)	Torque per Unit Volume (T/V)
64	.31	779	16	.75	4	9.42	82.7
36	.37	928	12	1	3	7.07	131.26
20	.31	784	10	1.25	2	3.93	199.49
14	.35	890	8	1.5	1.75	3.61	246.54

Table 13: Helical Gear Specifications with Pressure Angle of 14.5

Teeth	Power (HP)	Torque (lb-in)	P – Normal P (Teeth/in)	Face Width (in)	Diameter (in)	Volume (in^3)	Torque per Unit Volume (T/V)
30	.32	818	10 – 14.14	.875	3	6.19	132.15
24	.34	862	8 – 11.31	.75	3	5.3	162.64
16	.29	740	8 – 11.31	1	2	3.14	235.67
10	.3	758	6 – 8.48	1	1.67	2.19	346.12
10	.38	948	6 – 8.48	1.25	1.67	2.74	345.99

Table 14: Top Level Testing Summary

Experiment/Test	Relevant DRs	Testing Equipment Needed	Other Resources
Exp 1 – Device Weight Check	**ER2** – Less than 15 lb	Scale	
Exp 2 – Attachment Verification	**CR5** - Ensure standard attachment above and below	Lamination plate, Female pyramid adapter	
Exp 3 – Power Usage Test	**CR4** – Battery should last throughout the day **ER 7** - Last 1 hour of use	Multimeter/Power supply Weights Mounting System Camera	Arc Lab
Exp 4 –ROM Test	**ER4 -** (- 20°) to 135° sagittal ROM	IMU reading computer	
Exp 5 – Static Stand Test	**CR1** – Support 90 kg user	Bypass Support or rail for safety Scale Lower leg prosthesis	Arc Lab
Exp 6 – Stand to Sit Test	**CR7** – Stand to sit	Chair Rail/Support Bypass Camera	Arc Lab
Exp 7 – Sit to Stand Test	**CR6** – Sit to stand	Chair Rail/Support Bypass Camera	Arc Lab
Exp 8 – Motor Torque Performance Check	**ER5** – Torque of 66.2Nm	Mounting System Weight-tension system Camera	Arc Lab
Exp 9 – Motor Cadence Performance Check	**ER6** – Cadence of 1.25 steps per second	Mounting System Weight-tension system Camera	Arc Lab

Table 15: Static Stand Results

Trial	Sound Leg Load (lb.)	Prosthetic Leg Load (lb.)	Load difference (%)
1	114	82.4	16.1
2	105	95.2	4.9
3	93.1	106.8	-6.8%